CHEMICAL REVIEWS

REVIEW

pubs.acs.org/CR

MALDI Imaging of Lipid Biochemistry in Tissues by Mass Spectrometry

Karin A. Zemski Berry,[†,§] Joseph A. Hankin,[†,§] Robert M. Barkley,[†] Jeffrey M. Spraggins,[‡] Richard M. Caprioli,[‡] and Robert C. Murphy*[,†]

[†]Department of Pharmacology, University of Colorado Denver, Mail Stop 8303, 12801 East 17th Avenue, Aurora, Colorado 80045, USA

[‡]Department of Biochemistry and Mass Spectrometry Research Center, Vanderbilt University, 9160 MRB 3, 465 21st Avenue South, Nashville, Tennessee 37232, USA

CONTENTS

1. INTRODUCTION

As a result of recent advances, remarkable images revealing the distribution of complex lipids in tissues are now generated by matrix-assisted laser desorption/ionization imaging mass spectrometry (MALDI IMS). Lipids are amphipathic biomolecules with hydrophobic structural characteristics made by either an initial anion thioester condensation reaction (fatty acid synthase) or by carbocation condensation of branched-chain pyrophosphate intermediates (isoprene pathway).[1] Lipids play essential roles in cellular function including the self-assembly of phospholipids to form the constitutive outer and inner membrane bilayer of every living cell. Specific components of these membrane phospholipids include species that contain esterified arachidonate that can be enzymatically released to a free acid and transformed to potent signaling molecules (prostaglandins, leukotrienes) with myriad biological effects. The lipid cholesterol is an essential component of bilayer membranes that has a complicated, yet highly regulated biosynthesis. Elevation of cholesterol levels (predominantly as cholesteryl esters) in blood has been implicated in heart disease and is commonly monitored in consideration of human health. Some lipid molecules play the central role in biochemical energy storage in the form of triacylglycerol molecules stored in lipid bodies within almost all cells.

Mass spectrometry has historically been a tool of choice in biochemical studies of lipids. The sensitivity and specificity of mass spectral data are useful to sort out the complexity of lipid structures to begin to follow biological changes. While techniques such as fluorescence confocal microscopy or the ability to engineer proteins that can be expressed in cells with fluorescent tags have become the mainstream of modern biochemical research, such techniques are not amenable to most lipids because of the relatively small size of the lipid molecules and the dynamic nature of their structure in the cell. Recent developments in MALDI IMS have merged specificity of lipid identification with two-dimensional molecular mapping to enable biochemical studies of lipids across regions of a biological tissue.

Several significant reasons for the success of MALDI IMS applied to lipid imaging have emerged. The first is the high abundance of various lipids in biological tissues because these hydrophobic molecules constitute the external and internal defining membranes of each cell. These membranes are almost exclusively bilayers composed of phospholipids, sphingolipids, and cholesterol that are closely packed in high local concentrations to render the membrane only semipermeable to water. A second reason is that many lipids, e.g., phospholipids, are already ionized as either phosphate anions or nitrogen-centered cations and generate abundant positive or negative ions during the MALDI process. An equally important factor in the success of

Special Issue: 2011 Lipid Biochemistry, Metabolism, and Signaling

Received: July 25, 2011
Published: September 26, 2011

MALDI IMS of lipids is that the molecular weight of these biomolecules is generally below 1 000 Da, which is an optimal mass range for the most sensitive operation of modern mass spectrometers. Additionally, this low molecular weight facilitates diffusion of lipids into a matrix crystal driven by the high concentration of the lipid within the microstructure of the tissue.

Because of these fundamental factors coupled with the exciting potential of MALDI IMS, lipid molecules have been frequently used as examples for the advancement of IMS methodology and instrumentation. Research groups that utilize secondary ion mass spectrometry (SIMS) imaging have embraced lipid biochemistry by moving from inorganic applications to biological applications, development of larger particle size beams, and demonstrations of submicrometer lateral resolution.[2,3] Similar development and implementation of instrumentation for MALDI IMS has leveraged lipid diversity, abundance, and contrast in rodent brain samples to achieve advancements in technology.[4−8] The development of different matrices useful for MALDI IMS,[9−16] different methods of matrix application,[17−23] and different matrix modifiers[24,25] have been employed in MALDI IMS experiments to establish the value and parameters of these method modifications for lipid analysis.

Advances in biology have been a direct result of our ability to observe biochemical events at the micrometer and submicrometer regimes within a tissue. Having a sensitive technique that reveals molecular structure information about specific lipids in a tissue with 10−50 μm resolution and provides information relative to concentration of that lipid has already provided insight into lipid biochemistry at the tissue level. Because lipids are products of complex, intertwined enzymatic processes, MALDI IMS data reveal the integrated solution to complex reaction pathways that define the living cell in terms of lipid biochemistry. It has become apparent to a host of scientists converging into the use of MALDI IMS from fields as diverse as neuroscience, chemistry, and instrument development that there is a richness and complexity of lipid biochemistry suggested by the exquisite, molecule-specific MALDI images created in the course of developing this technology. Many reviews have focused on the technological developments of MALDI IMS of lipids with respect to the issues mentioned above.[2,26,27] This review focuses on the lipid biochemistry revealed by MALDI IMS.

2. LIPID IDENTIFICATION

Unambiguous identification of a lipid from the molecular ion species desorbed during the MALDI IMS process can be quite challenging and in many cases is not possible. The information available from the imaging experiment in most, but not all, cases defines the molecular weight of the lipid based on the assumption of the ion being $[M+H]^+$, $[M+Na]^+$, $[M+K]^+$, or $[M-H]^-$. However, in some cases the ion itself may be a fragment ion of a larger lipid, such as in the case of m/z 369.3 from cholesterol (loss of OH), m/z 548 from a ceramide (loss of H_2O), and phospholipids, which can lose the polar headgroup to form a dehydrated diacylglycerol fragment ion. Thus, a critical first step in identification of the lipid is to check assumptions about the nature of the ion being considered.

The different classes of phospholipids are preferentially detected as either positive or negative ions depending on the headgroup. Phosphatidylcholine (PC) and sphingomyelin (SM) lipids contain quaternary amine groups and therefore a permanent positive charge and are readily detected in positive-ion mode. In fact, these lipids tend to suppress the detection of other phospholipids present in the sample when using positive ion mode.[28,29] To obtain MALDI IMS data for phosphatidylserine (PS), phosphatidylinositol (PI), phosphatidylglycerol (PG), PC, and phosphatidylethanolamine (PE) directly from tissue, negative-ion mode analysis can be used with an appropriate matrix, such as 9-aminoacridine or 2,6-dihydroxyacetophenone. Therefore, the spatial distribution of PE, PS, PI, PG, PC, and SM lipids can be obtained after both negative- and positive-ion MALDI IMS studies of adjacent tissue sections are performed.

2.1. Molecular Ion Species Information

The mass defect or fractional mass of the molecular ion species provides information about the elemental composition of the desorbed ion from the tissue. If the mass accuracy of the mass analyzer is better than 0.1 Da, then the mass defect is quite useful in distinguishing an ion as being derived from a lipid because these hydrophobic molecular species typically contain a large number of hydrogen atoms. Most modern mass spectrometers such as quadrupole-based mass analyzers readily achieve this level of mass measurement accuracy. However, high-resolution instruments such as the orbitrap, Fourier transform/ion cyclotron resonance (FT-ICR), and the advanced time-of-flight analyzers (TOF) are capable of much better mass accuracy and resolution. There are 83 hydrogen atoms present in the $[M+H]^+$ of PC(34:1) at m/z 760.5860 that has an elemental composition of $C_{42}H_{83}NO_8P$. The mass of the hydrogen atoms contributes 83.6494 Da to the final mass of this ion because hydrogen atoms have an exact mass of 1.007825 Da. Most lipids display a significant mass defect relative to ions derived from peptides or endogenous metabolites. If a sufficient mass accuracy can be measured for the molecular ion species, then it is possible to calculate the elemental composition of the tissue-derived ion directly (see below).

Additional information present in the molecular ion species is the abundance of the carbon-13 isotope 1 Da higher. Naturally occurring carbon contains ~1.1% as the ^{13}C isotope. As a result, the PC(34:1) ion in the above examples, containing 42 carbon atoms, will appear with a ^{13}C isotope peak at m/z 761.5895 and abundance of 46% compared to the abundance of the monoisotopic ion at m/z 760.5850. This PC(34:1) example illustrates how attention to the molecular ion species can aid in identifying a desorbed lipid ion from a tissue due to a high mass defect and high abundance of ^{13}C due to the large number of carbon atoms present compared to other endogenous biomolecules that might be desorbed in the MALDI IMS experiment.

2.2. High-Resolution Analysis

The elemental composition of a lipid-derived ion in an imaging experiment can be determined if the experiment is carried out at high mass resolution and mass accuracy. Mass accuracy is the difference between the theoretical value of the ion mass and the measured mass. High-resolution mass spectrometers including TOF, orbitrap, and FT-ICR with mass accuracies typically below 20,[30] 3,[31] and 1 ppm,[32] respectively, allow the exact mass of ions to be determined within errors at the fourth or fifth decimal place. Once the accurate mass measurement of the ion has been recorded, the value is used to generate a possible elemental formula list using input of total numbers of carbon, hydrogen, oxygen, nitrogen, phosphorus, and sulfur atoms that fall within the error tolerances permitted between measured m/z and theoretical m/z. The possible matches for the elemental composition of an m/z are reduced with higher mass accuracy,

which is how mass spectrometers with high mass resolution can improve the confidence of a lipid identification. In addition to providing more precise mass accuracies, high mass resolution can be essential for maximizing the information collected from MALDI IMS experiments. Performing MALDI directly off-tissue produces inherently complex spectra with, in many cases, numerous chemical species giving rise to the signal at any given nominal mass. The chemical complexity, particularly in the typical lipid mass range (<1500 Da), is due to the large number of endogenous compounds related to the tissue as well as matrix-related clusters and adducts. The inability to resolve nominally isobaric ions can be problematic for IMS experiments in that resulting ion images could be misleading if the overlapping ions have different spatial distributions. In this case, the data from what seems to be a single ion would represent effectively a merged image of multiple ions. Recently, high-performance mass analyzers, including the FT-ICR and orbitrap, have been used for MALDI IMS experiments.[31,124,126,131,134] Each of these studies has demonstrated the utility of high mass resolution (>100 000 resolving power) for imaging mass spectrometry. Smith and co-workers demonstrated the ability to resolve two species at m/z 806.511 (PE(38:4)+K^+ or PC(35:4)+K^+) and m/z 806.566 (PC(36:3)+Na^+) during a MALDI imaging experiment from rat brain using a 7 T MALDI FT-ICR mass spectrometer.[134] Although accurate mass measurements are a powerful tool in the characterization of specific lipids, they are not sufficient for an unambiguous identification, mainly due to the existence of the many isomeric lipids possible in a tissue. A positive $[M+H]^+$ ion observed at m/z 782.5699 could be from either PC(16:0/20:4) or PC(18:2/18:2) because these are isomers that have the same elemental composition.

2.3. Collision-Induced Dissociation (Positive Ions)

Information about a specific lipid ion in terms of structural assignment requires additional experiments that are often performed separately from the image acquisition. One of the most powerful methods involves collisional activation of target ions desorbed from the tissue in both the positive and negative ion mode to provide structural insight. Most lipids yield useful collision-induced dissociation (CID) spectra,[33] and specific examples here will center on the CID behavior of glycerophospholipids (PL) because these lipids typically are the most abundant desorbed ions in MALDI IMS. One of the main fragmentation pathways of PL during CID in the positive ion mode is cleavage of the phosphate−glycerol bond, which results in the elimination of the polar headgroup as a neutral or charged species.[34] CID of the $[M+H]^+$ of a phosphatidylcholine lipid results in a phosphocholine ion at m/z 184, which is characteristic of diacyl, ether, and plasmalogen PC lipids, as well as sphingomyelin lipids.[44] For imaging experiments carried out in an ion trap mass spectrometer, this ion is not observed because of an instrument-specific limitation, in that many commercial quadrupole ion traps cannot hold low mass ions in the trap when high mass ions are trapped. Nonetheless, the ion at m/z 184 is the quintessential diagnostic ion of the phosphocholine polar headgroup. This ion reveals that the lipid is choline containing; if the precursor $[M+H]^+$ is observed at an even mass-to-charge ratio (nitrogen rule), it is likely a PC, and if the observed $[M+H]^+$ has an odd mass-to-charge ratio, the ion is likely derived from a SM. The fatty acyl groups can only be determined as total number of fatty acyl carbon atoms (CN) and total number of double bonds (DB) from the molecular weight. A common abbreviation to define the PC molecular species in imaging studies is PC(CN:DB).[35] There is currently no information in any imaging experiment, including high-resolution measurements, that defines the position of double bonds, the exact chain length of each fatty acyl group, or the assignment of fatty acyl groups as *sn*-1 or *sn*-2 based solely on the observed molecular ion species and CID of the PC positive ion.

Because sodium and potassium ions are abundant in biological systems, $[M+Na]^+$ and $[M+K]^+$ cations of PC and SM lipids are also observed directly from tissue samples. The fragmentation ions observed upon collisional activation of both $[M+Na]^+$ and $[M+K]^+$ of PC and SM lipids include neutral loss of trimethylamine (59 Da) and neutral loss of phosphocholine (183 Da).[36] Additionally, abundant product ions are observed in the CID spectra of $[M+Na]^+$ and $[M+K]^+$ of PC and SM lipids at m/z 147 and 163, respectively, which correspond to the sodiated or potassiated cyclic 1,2-phosphodiester ion.[37] Some research groups have added lithium salt with the matrix to produce lithiated PC ions from tissues because the CID of $[M+Li]^+$ of PC molecular species results in structurally relevant product ions that are indicative of the fatty acid chains esterified to the glycerol backbone of PC lipids.[24] In two studies, 2,6-dihydroxyacetophenone matrix was modified with 100 mM lithium chloride, and this mixture was applied onto rat brain[38] and mouse embryo implantation sites.[39] In a recent study, many different lithium salts, including lithium citrate, lithium acetate, lithium trifluoroacetate, lithium iodide, and lithium chloride, were evaluated at a concentration of 1−2 mg/mL. It was established that the best results were observed when lithium trifluoroacetate was mixed with α-cyano-4-hydroxycinnamic acid matrix and sprayed onto a rat brain section.[24] The lithiated PC lipids were collisionally activated directly from the tissue, and structural information that enabled the identification of the acyl groups esterified to the glycerol backbone of PC lipids was obtained. This approach is based on the studies of the CID of $[M+Li]^+$ of PC lipids formed by electrospray ionization (ESI) and results in neutral loss of free fatty acids, neutral loss of lithiated free fatty acids, and neutral loss of trimethylamine and the fatty acids.[40]

Additionally, headgroup information about PE and PS lipids can be obtained by positive ion CID, although these species are more easily detected as negative ions in MALDI IMS. CID of the $[M+H]^+$ of diacyl-PE and ether PE lipids results in the neutral loss of the phosphoethanolamine headgroup (141 Da), whereas the CID of sodiated PE lipids yields the neutral loss of vinyl amine $[M+Na-43]^+$, neutral loss of phosphoethanolamine $[M+Na-141]^+$, and neutral loss of sodiated phosphoethanolamine $[M+Na-163]^+$.[41] Additionally, product ions at m/z 164 (sodiated phosphoethanolamine), m/z 146 (dehydrated and sodiated phosphoethanolamine), and m/z 121 (loss of aziridine from sodiated phosphoethanolamine) are observed in the CID spectra of $[M+Na]^+$ of PE lipids.[42] These types of product ions have been observed from sodiated PE species directly from brain and liver tissues.[15] CID of PS lipids also results in headgroup specific fragment ions. The major product ion in the CID spectra of $[M+H]^+$ of PS lipids results from the neutral loss of the phosphoserine headgroup (185 Da). The CID of $[M+Na]^+$ of PS lipids was found to result in four major fragment ions corresponding to the neutral loss of serine (87 Da), neutral loss of phosphoserine (185 Da), and neutral loss of sodiated phosphoserine (207 Da), as well as a dominant fragment ion observed at m/z 208, which corresponds to sodiated phosphoserine.[43] These fragment ions were observed for sodiated PS molecular species directly from

brain and liver tissues.[15] Thus, the information obtained from positive ion mode CID allows the determination of the PL polar headgroup, alkali attachment ions, and molecular weight. Also, this information enables calculation of the total number of acyl carbon atoms and double bonds.

2.4. Collision-Induced Dissociation (Negative Ions)

The CID behavior of phospholipids that generate abundant negative molecular ion species in MALDI IMS (PE, PS, PI, PA, and PG) yields product ions characteristic of the fatty acyl groups esterified at the *sn*-1 and *sn*-2 positions of the glycerol backbone.[44] There has been some suggestion that it is possible to determine the exact site of esterification of each fatty acid because the most abundant carboxylate anion generally observed in the negative ion CID spectrum is derived from the *sn*-2 position of the phospholipid.[45] Additional minor ions in the CID spectra of PE, PS, PI, PA, PG, and PC lipids include the loss of a neutral ketene from the *sn*-2 fatty acyl substituent and loss of the *sn*-2 neutral carboxylic acid.[44] In addition, product anions indicative of certain phospholipid classes are also observed upon CID of $[M\text{-}H]^-$. Several ions that are unique to PI lipids, including m/z 223, 241, and 297, which are characteristic of the phosphoinositol headgroup,[46] originally were observed in ESI but are also found in MALDI IMS (see below). Product ions observed in the negative ion CID mass spectra of PS lipids include the loss of serine $[M\text{-}H\text{-}87]^-$ and the loss of serine and the *sn*-2 fatty acid $[M\text{-}H\text{-}87\text{-}R_2COOH]^-$.[47] The carboxylate anion and the neutral loss of each carboxylic acid are present in the negative CID spectra of PE, PS, PI, PG, PA, and PC lipids and are informative ions that can be used to identify the fatty acyl substituents that are esterified at *sn*-1 and *sn*-2.

2.5. Collision-Induced Dissociation (Other Lipids)

In addition to phospholipids, triacylglycerols (TAGs), ceramides, sulfatides (ST), and cardiolipin (CL) have also been observed directly from tissues, and their CID behavior permitted some level of structural identification. TAGs are typically observed in MALDI IMS as $[M+Na]^+$ ions, and the CID of these lipids produce two major types of ions $[M+Na\text{-}RCOOH]^+$ and $[M+Na\text{-}RCOONa]^+$.[48] Ceramides can be observed directly in tissue either as $[M+H]^+$ or $[M\text{-}H_2O+H]^+$ ions and during CID undergo amide bond cleavage with neutral loss of the fatty acid and water to yield an ion at m/z 264.[49] Sulfatide lipids have been observed directly in tissues as $[M\text{-}H]^-$, and product ions corresponding to the neutral loss of the long-chain base as an α,β-unsaturated aldehyde and loss of fatty acid as a neutral ketene were observed in the negative ion CID spectra, along with product ions at m/z 259, 257, and 241 that are derived from the 3-sulfogalactosyl group. However, the negative ion CID spectra of sulfatide lipids are dominated by m/z 97, which corresponds to a $[HOSO_3]^-$ ion from ESI data[50] as well as from MALDI IMS.[37] Finally, the negative ion CID spectra of cardiolipin molecules contain product ions resulting from the elimination of the fatty acid chains as carboxylate anions[51] in addition to fragment ions that include phosphatidic acid (PA) and dehydrated phosphatidylglycerol.[52]

2.6. Other Mass Spectral Structural Methods

Relative to lipid structures, but often underappreciated, is the issue of position and geometry of double bonds in fatty acyl chains. Traditional CID data do not provide any information concerning these structural features and typically the position of unsaturation in the fatty acyl group is assumed only on the basis of the most common fatty acids that naturally occur. This can be an incorrect assumption considering that lipids differing only in double-bond position can have different biochemical properties,[53] and detailed analysis of most lipid-derived fatty acids can reveal the occurrence of isomeric fatty acids such as 18:1 (oleic, *n*-9 and vaccenic, *n*-7) and 16:1 (palmitoleic, *n*-9 and sapienate, *n*-10).[54] Recently, Blanksby and co-workers developed a technique to directly assess double-bond location in phospholipids using reaction with ozone and CID of ozone-reacted ions formed in the collision cell (OzID).[55] The reaction of an unsaturated lipid ion with ozone yields two product ions, an aldehyde ion and a Criegee ion, for each carbon−carbon double bond in the lipid. These aldehyde and Criegee product ions of OzID are diagnostic of the position of unsaturation of the mass-selected lipid ion. For example, OzID of a phospholipid containing an *n*-9 fatty acid results in neutral loss of 110 and 94 Da from the precursor ion, which is the aldehyde and Criegee product ions that are indicative of an *n*-9 fatty acid. This technique has not yet been applied to structurally identify lipids directly off-tissue; however, when OzID is used along with conventional CID, positional assignment of double bonds in a lipid ion of interest can be determined. More recently, the use of a tandem ion mobility mass spectrometer system was suggested to generate data relevant to the double-bond position by using ion mobility to separate fragment ions derived from CID of the positive molecular ion of PC.[56] In theory, the position of double bonds of the fatty acids of lipids can be determined in the positive or negative ion mode from phospholipid ions desorbed from a tissue.

3. ION ABUNDANCE AND LOCAL LIPID CONCENTRATION

MALDI IMS depicts regional localization of specific lipids in many different types of tissues. The validity of these MALDI images, specifically the relationship between MALDI IMS ion intensity and the amount of the lipid actually present in the tissue, although visually intuitive, is in reality affected by a complex combination of ion chemistry, tissue structure, lipid location within the cells of the tissue, and water and salt content. The sample ablation process in MALDI desorbs a complex mixture of biological molecules including lipids, proteins, peptides, nucleic acids, and metabolites from a tissue, and the prominent molecules ionized in MALDI IMS in the mass range m/z 500−1000 are lipids. However, within this group of molecules lies complexity due to mixtures of polar head groups, isomeric configurations, salt adducts, and isobaric molecules. Additionally, PC molecules suppress the ionization of other lipids in positive ion MALDI ionization,[28] and in negative ion mode, matrix adducts of PC complicate and interfere with the spectra of phospholipids that ionize as $[M\text{-}H]^-$ species.[29] The matrix used for MALDI IMS affects the ionization of specific lipids as shown in the MALDI TOF analysis of inositol tri- and hexaphosphate molecules, which were readily visible using 9-aminoacridine as matrix and not visible when using α-cyano-4-hydroxycinnamic acid.[57]

A recent study contrasted regional intensities generated by MALDI IMS of rat brain to measured amounts of phosphatidylcholine molecules in the same regions analyzed through microdissection, lipid extraction, and ESI/MS.[58] This study supported the hypothesis that, within a singular class of lipid (e.g., phosphatidylcholine) and similar tissue types, the intensity of lipid molecular species generated in positive ion MALDI

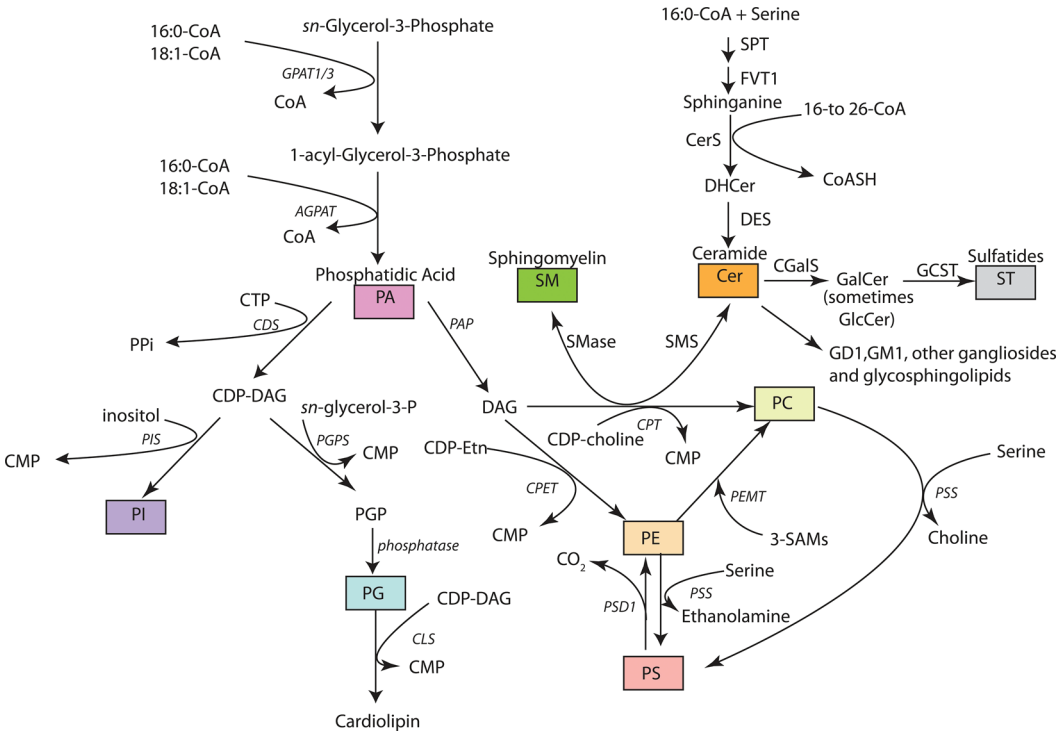

Figure 1. Schematic biosynthetic pathways for the major phospholipid (Kennedy pathway) and sphingolipid classes biosynthesized in mammalian cells and observed in MALDI IMS of mammalian tissues. The lipids in the boxes are the major lipid species that generate either positive or negative ions. Each class is populated with individual molecular species. Abbreviations of lipid classes follow the Lipid Maps suggested abbreviations. Abbreviations of enzymes indicated in the pathways are as follows: GPAT1/3, glycerol-3-P acyltransferase; AGPAT, acylglycerol-3-P acyltransferase; CDS, CDP-DAG synthase; PAP, phosphatidic acid phosphatase; CPT-CDP-choline, 1,2-diacylglycerol cholinephosphotransferase; PIS, PI synthase; SAMs, *S*-adenosylmethionine; CPET-CDP-Etn, 1,2-diacylglycerol ethanolaminephosphotransferase; PSD1/2, phosphatidylserine decarboxylase isoforms; CLS, cardiolipin synthase; PGPS, PG-P synthase; PSS, phosphatidylserine synthase isoforms; PEMT, phosphatidylethanolamine *N*-methyltransferase; GCST, GalCer sulfotransferase; CGlcS, glucosyl ceramide synthase; FVT1, 3-ketosphinganine reductase; DES, dihydroceramide desaturase; PAPS, phosphoadenosine phosphosulfate; CGalS, galactosyl ceramide synthase; SMS, sphingomylelin synthase; SMase, sphingomylenase; CerS, dihydroceramide synthase; and SPT, serine palmitoyltransferase.

IMS experiments does in fact relate to the quantity of molecules in a tissue sample. For example, MALDI IMS of PC(18:0/22:6) in brain tissue shows an increased intensity in the cerebellum of rat and mouse brain that was correlated with the ESI/MS measurements made in the next serial slice. Comparisons made between brain anatomical regions were more consistent when a particular phospholipid ion abundance observed in either the ESI or MALDI data sets was normalized to the common abundant phospholipid in that brain region, suggesting that MALDI IMS ion abundances are more accurately thought of as "relative amounts" rather than absolute amounts.[159] This implies that tissue structure specific effects are in play, affecting the ionization of lipids during MALDI IMS. These results deter from using intensity alone as a quantitative measure of lipid amount at a specific anatomical site.

Regional intensity contrasts between top and bottom halves of MALDI images for 8-week-old mouse embryos were compared with ESI/MS/MS measurements of the same lipids for an assortment of PC molecules measured in positive ion mode, and both PE and PI molecules measured in negative ion mode.[39] There was corroboration between abundance measurements between the two techniques, supporting the concept that the intensity of an ion in MALDI IMS is consistent with the relative amount of the lipid imaged when limited to comparison between specific classes.

4. GLYCEROPHOSPHOLIPIDS

The phospholipids constitute a major class of lipids present in all cells. They are significant components of cellular membranes and are typically asymmetrically distributed across the membrane bilayer. Specifically, PC is in higher abundance in the outer leaflet of the bilayer of the normal cell outer membrane defining the cell, while aminophospholipids such as PS and PE, as well as PI, are found in highest concentration on the inner leaflet.[59] These lipids occur in tissues as families of closely related molecules that differ by the fatty acyl substituent esterified to the *sn*-1 and *sn*-2 oxygen atoms of the common glycerol backbone and are termed "molecular species."

These molecular species arise from both de novo synthesis and from phospholipid remodeling events. For example the PC(16:0/16:0) can be synthesized from palmitic acid CoA ester (made from acetate by fatty acid synthase), which is esterified to glycerophosphate, then phosphate removed to form the diacylglycerol (1,2-dipalmitoylglycerol). The addition of the choline polar headgroup to the diacylglycerol takes place via the intermediate cytidine diphosphate diacylglycerol choline (CDP-choline) and the enzyme CDP-choline:1,2-diacylglycerol cholinephosphotransferase to form the PC in what is called the Kennedy biosynthetic pathway (Figure 1).[60] Other pathways of PC synthesis can result by way of sequential methylation of preformed PE.[61] PE lipids are de novo synthesized in a similar

dx.doi.org/10.1021/cr200280p |*Chem. Rev.* 2011, 111, 6491–6512

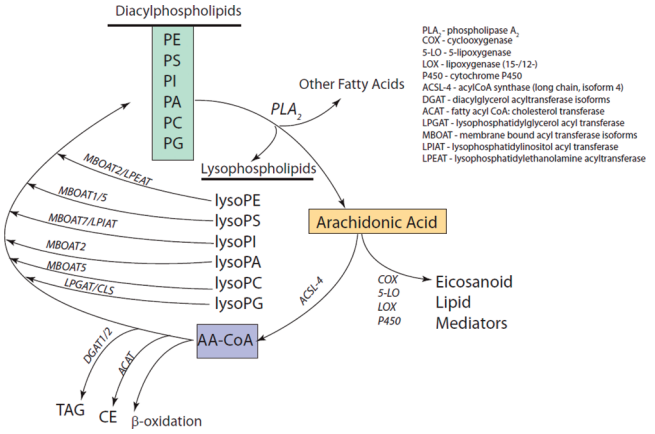

Figure 2. Remodeling of fatty acyl groups of common glycerophospholipids using arachidonic acid as an example of the modified Lands' pathway responsible for diversity of phospholipid molecular species observed in MALDI IMS of tissues. Arachidonic acid released from phospholipids by phospholipase A_2 (PLA_2) is primarily converted into arachidonoyl CoA thioester. A small fraction of free arachidonic acid is available for lipid mediator biosynthesis into eicosanoids. The arachidonoyl CoA is substrate for transferases to re-esterify neutral lipids back into phospholipids by acylation of lysophospholipids. Other acyltransferases may be involved in addition to those indicated. Arachidonate degradation by β-oxidation proceeds by the CoA ester intermediate.

fashion from diacylglycerol. One interesting variant in synthesis is ether phospholipid biosynthesis, which occurs primarily for PE and leads to the occurrence of both 1-*O*-alkyl ether PE and PC species and their vinyl ether analogues known as plasmalogens.[62] In contrast, phosphatidylinositol is synthesized de novo from CDP-diacylglycerol and inositol catalyzed by phosphatidylinositol synthase.[63] Phosphatidylserine can be synthesized from serine and CDP-diacylglycerol by a de novo pathway in lower organisms and by base exchange of serine for choline in PC (PS synthase I) or ethanolamine in PE (PS synthase II).[64]

The observed diversity in all phospholipid molecular species in cells cannot be explained by these de novo pathways but is a result of phospholipid remodeling of fatty acyl groups in what has been termed the Lands' pathway (Figure 2).[65] For example, fatty acyl groups can be removed from de novo synthesized PC by the action of phospholipase A_2 and phospholipase A_1 to form lysoPC.[66] Expansion of PL diversity then takes place when different lysoPLs are esterified with the coenzyme-A ester of cellular fatty acids, catalyzed by the action of lysophosphatidylglycerol acyl transferases (LATs). These LATs have different specificities for fatty acyl CoA esters as well as lysoPL species.[67] The result is a very substantial mixture of molecular species of PL that differ in fatty acyl group. The structural diversity in the fatty acyl group also includes unsaturation at specific sites of the fatty acyl chain into families of *n*-5, *n*-7, and *n*-9 monounsaturated acyl groups, where the number represents the position of the double bond relative to the terminal carbon atom. Although normal biochemistry generates cis double-bond isomers, trans isomers can be found in phospholipids because of their ingestion or oxidative stress in a tissue. For polyunsaturated fatty acyl groups, biosynthesis yields homoconjugated, all-cis isomers where the terminal chain double bond is typically *n*-6 or *n*-3. In lower animal species, even greater diversity exists with branched chain fatty acyl groups as well as other structural motifs.[68] As a result of oxidative stress due to disease or other pathologic events, the polyunsaturated fatty acyl groups can be oxidized to many different species of varying complexity from simple addition of an oxygen atom to form a conjugated diene hydroperoxide[69] to very complex esterified isoprostanes.[70] The challenge of imaging mass spectrometry is to identify those observed ions with unusual tissue distribution compared to other PLs (see section 2) and to understand the event that leads to these unique spatial distributions.

4.1. Phosphatidylcholine

The major phospholipid present in cell membranes of most organisms is PC, which accounts for 40−50% of the total phospholipid pool.[71] In addition to PC lipids serving a crucial role as the main structural element of biological membranes, these PC lipids are also precursors to signaling molecules. Many phospholipases (PLA_1, PLA_2, PLC, and PLD) target PC lipids and generate unique signaling mediators that include phosphatidic acid, diacylglycerol, lysoPC, platelet-activating factor, and arachidonic acid.[72] The major subclass of PC lipids present in most tissues is diacyl, but alkylacyl and alkenylacyl PC lipids are also found. In fact, in neutrophils, eosinophils, and macrophages, alkylacyl PC lipids account for 30−70% of the cellular PC[73,74] and alkenylacyl PC lipids are present in relatively high abundance (20−30%) in heart tissue.[75]

PC lipids are typically observed in MALDI IMS as positive ions from *m/z* 678.5 (PC(28:0)) to *m/z* 902.7 (PC(44:0)), and lysoPC molecular species are observed as positive ions from *m/z* 468.3 (14:0 lysoPC) to *m/z* 580.4 (22:0 lysoPC). The PC polar headgroup is a quaternary ammonium ion and thus always ionized. MALDI of PC yields abundant positive ions as $[M+H]^+$ where the additional proton neutralizes the phosphate anion. The normal distribution of ions observed in the MALDI imaging experiment often is dominated by PC molecular species, but differences in ion abundance of some species seem to be related to different lipid biochemistry in specific anatomical regions. For example, MALDI IMS can reveal unique spatial distributions of polyunsaturated fatty acid containing PC in the brain (Figure 3), which suggests anatomical compartmentalization of specific fatty acyl groups.[156] Table 1 lists those $[M+H]^+$, $[M+Na]^+$, and $[M+K]^+$ PC molecular species that have been identified by CID in various tissues. For PC lipids these diagnostic ions are *m/z* 184 (from $[M+H]^+$ PCs), neutral loss of 183 (from $[M+Na]^+$ and $[M+K]^+$ PCs), neutral loss of 59 (from $[M+Na]^+$ and $[M+K]^+$ PCs), and the sodiated or potassiated cyclic phosphate ion as described above in section 2.

Phosphocholine lipids are the most prevalent class of lipids that ionize in positive ion MALDI IMS of most tissues, and typically a mixture of $[M+H]^+$, $[M+Na]^+$, and $[M+K]^+$ ions are observed for each PC molecular species and can lead to complicated MALDI mass spectra directly off-tissue. Therefore, some research groups add alkali metal salts during matrix deposition to simplify the MALDI mass spectra off-tissue and increase the sensitivity by merging the $[M+H]^+$, $[M+Na]^+$, and $[M+K]^+$ of a single lipid into one alkali metal ion. For example, Sugiura and Setou added 10 mM potassium acetate along with 2,5-dihydroxybenzoic acid matrix to a rat kidney section,[25] which resulted in the presence of only $[M+K]^+$ PC ions on the tissue and allowed the localization of PC lipids in the rat kidney slice to be determined by MALDI IMS. Additionally, lithium trifluoroacetate was found to be an excellent matrix additive to α-cyano-4-hydroxycinnamic acid, leading to the observation of mainly $[M+Li]^+$ lipid-derived ions from rat brain tissue during the

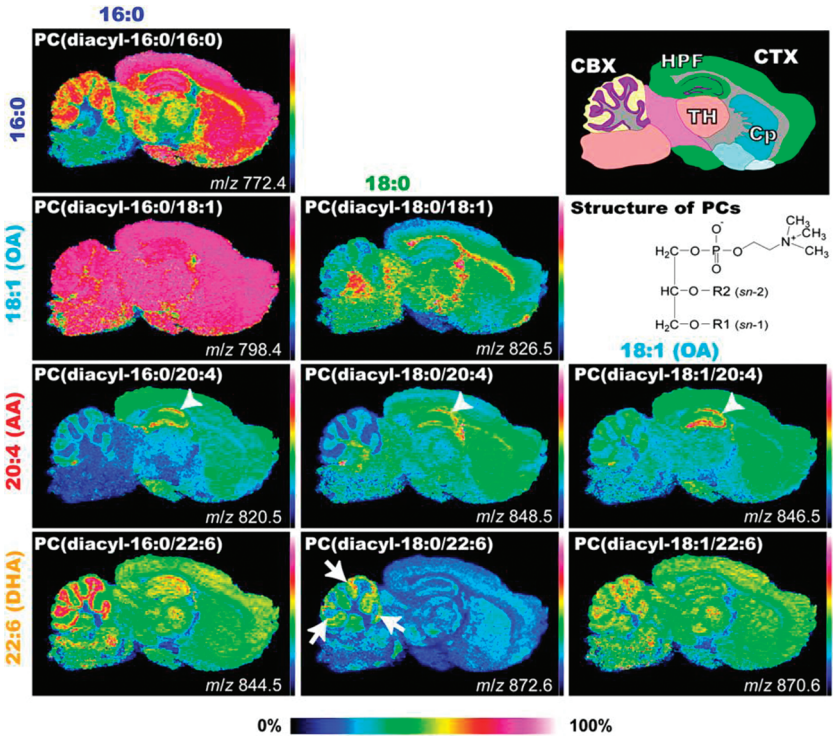

Figure 3. Differential distribution of PC molecular species in sagittal mouse brain sections. MALDI IMS spectra of a brain section simultaneously identified the heterogeneous distributions of several PCs. Schema of the mouse brain sagittal section and ion images of PCs obtained by IMS are shown. Ion images of PCs are arranged according to their fatty acid (FA) composition. PCs with identical FA compositions at the *sn*-1 position are arranged lengthwise, whereas those with identical FA compositions at the *sn*-2 position are arranged sideways. The structures of PCs are also presented. Among the PCs, arachidonic acid-PCs showed characteristic localization in the hippocampal cell layers (arrowheads). Among docosahexaenoic acid-containing species, two abundant species, PC(16:0/22:6) and PC(18:1/22:6), were commonly enriched in the granule layer of the cerebellum, whereas PC(18:0/22:6) showed a characteristic dotted distribution pattern near the cell layer (arrows). Abbreviations: CBX, cerebellar cortex; CP, corpus striatum; CTX, cerebral cortex; HPF, hippocampal formation; TH, thalamus. Reprinted with permission from ref 156. Copyright 2009 The American Society for Biochemistry and Molecular Biology.

MALDI IMS experiment.[24] The addition of lithium salt to tissue with matrix has the added benefit of enhancing the structural information obtained from CID as described previously.

In addition to simplifying lipid spectra by adding alkali metal salts, a washing protocol has recently been developed to remove salts and other complicating matrix ions.[138] This approach is more in line with traditional sample-preparation techniques for MS analysis of biological samples by using volatile buffers that not only displace endogenous salts but are also eliminated from the tissue under vacuum. Wang et al.[138] found that washing rat brain tissue sections with 150 mM cold ammonium acetate prior to matrix application enhanced signal from $[M+H]^+$ PC ions while eliminating PC salt adducts. The washing procedure was performed by simply dripping 1 mL of the cold wash solution over the tissue section and then drying the sample in a vacuum desiccator for 20 min prior to matrix application. Analysis of the wash runoff solution found no lipids to be present, suggesting that lipid delocalization is minimal using this technique.

Although the addition of alkali metals and washing with aqueous volatile salt solutions can simplify MALDI spectra, the information related to the endogenous alkali metal ion distribution in tissue can be lost. This was demonstrated in a study where MALDI IMS was used to examine the localization of lipids upon traumatic brain injury (TBI) in rat brain.[76] The MALDI IMS images of the $[M+H]^+$ and $[M+K]^+$ of PC(34:1) at m/z 760.6 and 798.6, respectively, revealed that these PC ions were less abundant in the injured region (Figure 4). Conversely, the distribution for the sodium adduct of PC(34:1) at m/z 782.6 (Figure 4c) indicated an increased intensity at the injured region. In addition, MALDI IMS of a more severe TBI injury displayed the same pattern of increased sodium and decreased potassium adducts related to the TBI, but deeper into the brain tissue. Because a dry sublimation method was used to deposit the matrix, the alkali metal ions present in the tissue during the TBI were preserved and the observed variability in alkali metal attachment was most likely a measure of relative alkali metal concentration differences between two regions. Therefore, the authors suggested that this altered alkali metal attachment to PC lipids in the injured region of the brain is a sensitive indicator of the events taking place at a molecular level. This change in PC alkali attachment ion was suggested to result from edema and influx of extracellular fluid likely through a loss of Na/K-ATPase caused by the TBI.

Negative ions can also be obtained from PC species but at a significant loss of signal. These $[M-15]^-$ ions correspond to loss of a methyl group from the quaternary ammonium form.[104] Images of negative ions from PC have not been reported.

4.2. Phosphatidylethanolamine

Phosphatidylethanolamine is the second most abundant mammalian membrane phospholipid and constitutes 20−30% of the total cell phospholipid.[71] PE lipids are present as diacyl,

Table 1. Positive Ion Phospholipid Molecular Species Identified by CID of Tissue-Derived Ions

this work m/z			structurally specific CID product ions (m/z)				
exp[b]	calc[c]	assignment	phosphocholine ion	sodiated or potassiated cyclic 1,2-phosphodiester	neutral loss of choline (NL 59 Da)	neutral loss of phosphocholine (NL 183 Da)	tissue[a, ref]
496.3	496.3403	PC(16:0/OH)	184				mu tongue,[151] mu embryo[137]
			184			313	rat brain[152]
520.3	520.3403	PC(18:2/OH)	184				mu tongue[151]
524.3	524.3716	PC(18:0/OH)	184				mu tongue[151]
703.4	703.5754	SM(d18:1/16:0)			644	520	mu tongue[151]
705.4	705.5910	SM(d18:0/16:0)	184				human lens[153]
725.5	725.5573	SM(d18:1/16:0)+Na		147	666	542	hu ovary,[13] mu lung,[88] hu placenta[154]
			184		666	542	hu liver[18]
731.5	731.6067	SM(d18:1/18:0)	184				rat brain[38]
734.6	734.5654	PC(32:0)	184				mu lung,[88] rat brain[38,24]
					675	551	mu tongue[151]
741.5	741.5313	SM(d18:1/16:0)+K	184	163	682		crustacean brain[155]
744.5	744.4946	PC(30:0)+K			685	561	mu brain,[156] hu brain[157]
753.4	753.5886	SM(d18:1/18:0)+Na			694	570	rat spinal cord[31]
756.6	756.5519	PC(32:0)+Na			697	573	mu retina,[158] rat brain,[38,16] rat spinal cord[31]
758.5	758.5654	PC(34:2)	184				mu liver[15]
					699	575	mu tongue[151]
760.6	760.5856	PC(34:1)	184				mu lung,[88] rat brain,[38,4] rat spinal cord,[160] mu brain[22]
					701	577	mu tongue[151]
769.5	769.5626	SM(d18:1/18:0)+K		163	710		rat brain[38]
770.5	770.5100	PC(32:1)+K			711	587	mu brain[156]
772.5	772.5259	PC(32:0)+K		163	713		rat kidney,[25] rat brain[38]
					713	589	mu retina,[158] mu brain[156]
			184	163	713	589	rat brain[14]
780.5	780.5519	PC(34:2)+Na		147	721	597	mu liver[15,161]
782.6	782.5675	PC(34:1)+Na		147	723	599	mu embryo,[137] mu lung,[88] rat brain[25]
					723	599	rat spinal cord,[31,161] rat brain,[7] mu retina[158]
	782.5654	PC(36:4)	184				mu lung,[88] rat brain[25]
					723	599	mu tongue[151]
	782.5466	PC(34e:2)+K		163	723	599	rat brain[25]
784.6	784.5856	PC(36:3)			725	601	mu tongue[151]
786.6	786.6012	PC(36:2)			727	603	mu tongue[151]
788.6	788.6157	PC(36:1)	184				rat brain,[38] rat spinal cord[160]
					729	605	mu tongue[151]
796.4	796.5259	PC(34:2)+K			739	615	mu brain[156]
797.5	797.5939	SM(d18:1/20:0)+K			738	614	hu brain[157]
798.5	798.5415	PC(34:1)+K		163	739	615	hu ovary,[13] rat brain,[38] rat brain[25]
					739	615	mu retina,[158] mu brain,[156,8] hu brain,[157] rat spinal cord[160,31]
				163	739		rat brain[152]
804.5	804.5519	PC(36:4)+Na		147	745	621	hu placenta[154]
					745	621	mu aorta[162]
806.6	806.5675	PC(36:3)+Na		147	747	623	mu lung[88]
	806.5694	PC(38:6)	184				mu lung[88]
					747	623	mu tongue[151]
810.6	810.5988	PC(36:1)+Na			751	627	rat spinal cord[16,31]
	810.6013	PC(38:4)			751	627	mu tongue[151]

dx.doi.org/10.1021/cr200280p |Chem. Rev. 2011, 111, 6491–6512

Table 1. Continued

this work m/z			structurally specific CID product ions (m/z)				
exp[b]	calc[c]	assignment	phosphocholine ion	sodiated or potassiated cyclic 1,2-phosphodiester	neutral loss of choline (NL 59 Da)	neutral loss of phosphocholine (NL 183 Da)	tissue[a, ref]
820.6	820.5259	PC(36:4)+K		163	761		hu ovary,[13] rat kidney[25]
					761	637	mu tongue,[151] mu brain,[156] hu brain[157]
				163	761	637	rat brain[25]
822.5	822.5415	PC(36:3)+K			763	639	hu brain[157]
824.5	824.5571	PC(36:2)+K			765	641	hu brain[157]
826.5	826.57281	PC(36:1)+K			767	643	mu brain[8,156]
					767		mu brain[163,164]
			184	163	767		mu brain,[23] crustacean brain[155]
				163	767		mu brain[22]
828.6	828.5513	PC(38:6)+Na			769	645	mu retina,[158] salamander retina,[165] mu tongue,[151] rat brain[7]
832.5	832.5832	PC(38:4)+Na			773	649	mu aorta[162]
834.6	834.6007	PC(40:6)			775	651	mu tongue[151]
			184				mu brain[22]
835.8	835.714	SM(d18:1/24:1)+Na			776	652	rat spinal cord[16,31]
837.5	837.6830	SM(d18:1/24:0)+Na			778	654	rat spinal cord[31]
844.6	844.5253	PC(38:6)+K		163	785		rat kidney[25]
					785	661	mu retina,[158] salamander retina[164] mu tongue,[151] mu brain[156]
846.5	846.5415	PC(38:5)+K			787	663	mu brain[156]
848.5	848.5572	PC(38:4)+K		163	789		rat kidney[25]
					789		rat spinal cord[31]
					789	665	mu brain[156]
856.6	856.5826	PC(40:6)+Na			797	673	mu tongue,[151] mu retina[158]
870.5	870.5409	PC(40:7)+K			811	687	mu brain[156]
872.5	872.5566	PC(40:6)+K			813	689	mu retina,[158] mu brain[156]

[a] Abbreviations: mu, mouse; hu, human. [b] Experimentally measured. [c] Calculated.

alkylacyl, and alkenylacyl molecular species, and as much as 70% of the PE in inflammatory cells and neurons contains an ether linkage. PE lipids can hydrogen bond to proteins through the ionizable primary amine located on the headgroup, and it is believed that PE exerts a lateral pressure in the membrane bilayer to stabilize membrane proteins in their optimal conformation. PE lipids play a role in membrane fusion and fission events,[77] which are thought to be related to the ability of PE to form hexagonal II phases in membranes. PE is also the precursor of anandamide, *N*-arachidonoylethanolamine,[78] which is a ligand for cannabinoid receptors in the brain. An additional characteristic of PE lipids is that the primary amine present on the PE lipid can react with aldehydes. For example, PE can react to form Michael adducts with the aldehydes that are products of oxidation of unsaturated fatty acids, such as 4-hydroxy-2(*E*)-nonenal.[79] Under conditions of oxidative stress in vivo, these compounds may influence the properties of membranes. Another example is Amadori products, which are formed from glucose adducted as a PE lipid Schiff base followed by rearrangement, that have been implicated in a number of disease states such as atherogenesis, diabetes, and aging.[80] Finally, all-*trans*-retinal-PE adducts are an important part of the visual cycle, and these products have been found to accumulate in retinal diseases.[81] PE lipids display a similar wide diversity of molecular species due to phospholipid remodeling and can be observed as positive $[M+H]^+$ ions from m/z 636.6 (PE(14:0/14:0)) to m/z 860.7 (PE(22:0/22:0)), as well as alkali attachment ions. PE $[M+H]^+$ ions are not as stable as the PC $[M+H]^+$ ions formed by MALDI and undergo facile loss of the polar headgroup $[M+H\text{-}141]^+$ to form a "diglyceride-like" cation.[33] This instability is similar for all phospholipids except PC and yields a "diglyceride-like" cation at the identical mass-to-charge ratio for each PL molecular species having the same fatty acyl groups esterified on the glycerol backbone. An example is the presence of m/z 579.5, which can arise from decomposition of $[M+H]^+$ during the MALDI imaging of PE(16:0/18:1), PI(16:0/18:1), or PS(16:0/18:1) present in the tissue. It is possible to confuse these ions, which can be observed in the MALDI mass spectra from tissue slices, with ions corresponding to the loss of water from true diacylglycerols that may be present in the tissue.

PEs are more typically detected as the negative ion $[M\text{-}H]^-$ in MALDI IMS experiments. These negative ions do not form alkali metal attachment ions, and thus the pattern of molecular species

dx.doi.org/10.1021/cr200280p |*Chem. Rev.* 2011, 111, 6491–6512

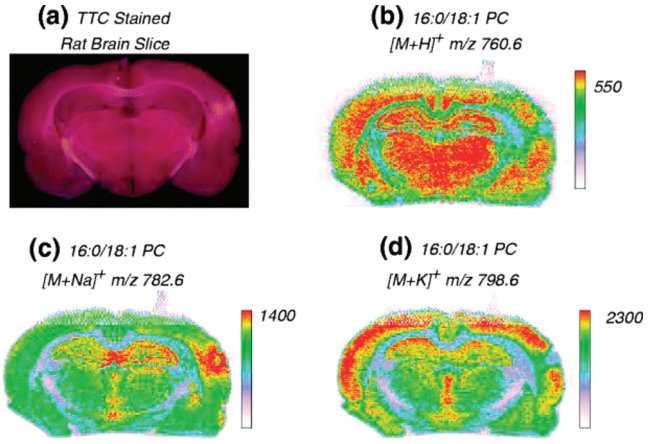

Figure 4. Rat brain sections from traumatic brain injury (TBI) model. (a) Tissue section stained with 2,3,5-triphenyltetrazolium chloride (TTC); (b) MALDI IMS representing PC(16:0/18:1) $[M + H]^+$ m/z 760.6; (c) MALDI IMS representing PC(16:0/18:1) $[M + Na]^+$ m/z 782.6; (d) MALDI IMS representing PC(16:0/18:1) $[M + K]^+$ m/z 798.6. Reprinted with permission from ref 76. Copyright 2011 American Society for Mass Spectrometry.

seen as negative ions is somewhat simpler than that of the positive ion PE or PC molecular species ions. The abundance of the PE negative molecular ion species is usually greater than for the corresponding positive ions, but in part this could be due to the instability of the positive ion or ion suppression by PC species in tissues. Another important feature is that collisional activation of $[M-H]^-$ from PE, as well as all other phospholipids, yields abundant and structurally relevant product ions corresponding to each fatty acyl group as a carboxylate anion and a loss of each fatty acyl group as a neutral ketene and neutral carboxylic acid. For most cases the loss of the *sn*-2 fatty acyl moiety is more abundant than the *sn*-1 group, which enables an assessment of the site of esterification along with identification of the fatty acyl groups themselves. The $[M-H]^-$ from PE generates excellent images of molecular species distributions. Table 2 lists the negative ions $[M-H]^-$ for specific PE molecular species that have been reported off-tissue.

Only a few detailed studies of PE distribution in tissues have been examined. In one example, MALDI IMS was used to characterize the spatial and temporal distribution of PE molecular species associated with mouse embryo implantation.[39] The negative ion MALDI images within implantation sites showed that distribution of PE, as well as PS, PI, and PG, changed markedly between distinct cellular areas during days 4−8 of pregnancy (Figure 5). MALDI IMS revealed that, by day 8, docosahexaenoate-containing PE lipids (confirmed by negative ion CID) were localized to regions destined to undergo apoptosis (AM pole), whereas oleate- and arachidonate-containing PE lipids were localized to angiogenic regions (M pole). The presence of these aforementioned fatty acids esterified to the glycerol backbone of PE lipids was confirmed by CID of ions of interest directly off-tissue. Prostaglandin signaling, resulting from $cPLA_2$ and COX-2 processing of arachidonic acid, participates in embryo attachment and uterine decidualization during embryo implantation. COX-2 expression localizes to the M pole above the ectoplacental cone (EPC), and the MALDI IMS of arachidonate-containing PE lipids revealed a strong correlation with $cPLA_{2\alpha}$ and COX-2 during embryo implantation. These MALDI imaging experiments revealed the dynamic complexity of PE lipid distributions in early pregnancy, signifying the importance of complex interplay of lipid molecules in uterine biology and implantation.

4.3. Phosphatidylserine

Phosphatidylserine is a minor membrane phospholipid that makes up 2−10% of the total phospholipids in a mammalian cell.[71] During the early phases of apoptosis, PS becomes externalized on the outside of the cell, and this surface exposure of PS stimulates phagocytes to engulf an apoptotic cell and to produce anti-inflammatory mediators.[82] It is thought that the exposure of PS on the outer membrane of cells undergoing apoptosis is promoted by reduced activity of the aminophospholipid translocase combined with increased scramblase activity. An additional biological function of PS is as a cofactor that activates several signaling proteins, such as protein kinase C.[83] In many tissues, polyunsaturated fatty acyl chains, primarily arachidonic and docosahexaenoic acids, are present at the *sn*-2 position of PS lipids.[84] This might be due to the expression of a specific LAT enzyme termed MBOAT5 that has a preference for acylation of lysoPS using arachidonoyl-CoA and other polyunsaturated fatty acyl CoA esters.[67] Additionally, this aminophospholipid does not have the wide diversity of molecular species that is observed for PE and PC in tissue. MALDI mages of PS are usually observed as negative ions and can range from m/z 734.5 (PS (14:0/14:0)) to m/z 902.7 (PS (22:0/22:0)). Table 2 lists the negative ions $[M-H]^-$ for specific PS molecular species that have been collisionally activated and identified in MALDI IMS studies.

MALDI images of PS lipids were also obtained in the embryo implantation study first mentioned in section 4.2,[39] and these images indicated that on day 8 of pregnancy oleate-containing PS lipids were localized to the M pole and linoleate-containing PS lipids were localized to the AM pole (Figure 5). The presence of these fatty acids in PS lipids was established by CID of the corresponding $[M-H]^-$ directly off-tissue.

4.4. Phosphatidylinositol

Phosphatidylinositol is an acidic lipid that constitutes 10−15% of total phospholipids in mammalian cells and is found in the inner leaflet of the plasma membrane.[71] Additionally, these lipids are precursors to polyphosphoinositol lipids (PIP, PIP_2, PIP_3) that are formed by the reversible phosphorylation of the inositol ring. These phosphatidylinositol-derived compounds play a key role in cell signaling and regulation, including intracellular calcium signaling, gene transcription, RNA editing, nuclear export, and protein phosphorylation.[85] PI molecular species are not as numerous and diverse as PE and PC molecular species. This is partly a consequence of a specific acyltransferase (MBOAT7) that incorporates arachidonate from arachidonoyl-CoA into lyso PI.[67] This results in the most abundant PI in many tissues being PI(18:0/20:4),[86] which is observed at m/z 885.5 in MALDI mass spectra directly off-tissue. Polyphosphoinositol lipids are products of PI kinases and play critical intracellular roles,[87] but they are of such low abundance that they have yet to be observed in imaging studies. PI lipids are observed as negative ions in the mass range from m/z 807.7 (PI(14:0/14:0)) to m/z 977.7 (PI(22:0/22:0)). Table 2 lists the negative ions $[M-H]^-$ for specific PI molecular species that have been collisionally activated directly off-tissue in MALDI IMS studies.

Table 2. Negative Ion Lipid Molecular Species Identified by CID of Tissue-Derived Ions

this work m/z			structurally specific CID product ions (m/z)			
exp[b]	cal[c]	assignment	fatty acyl ions	diagnostic headgroup ions	loss of R_2COO^- ($R_2CHC{=}O$)	tissue[a,ref]
599.3	599.3197	PI(18:0/OH)	283		315	mu embryo[137]
716.5	716.5228	PE(16:0/18:1)	281, 255			mu brain,[164] mu embryo[39]
722.5	722.5125	PE(16:0p/20:4)	303			mu brain[164]
726.5	726.5438	PE(18:1p/18:1)	281		444 (462)	mu brain[164]
728.6	728.5594	PE(18:0p/18:1)	281		(464)	mu brain[164]
742.5	742.5386	PE(18:1/18:1)	281		(478)	mu brain,[164] mu embryo[39]
		PE(18:0/18:2)	279, 283		(480)	mu embryo[39]
744.6	744.5543	PE(18:0/18:1)	283, 281		(480)	mu brain[164]
746.5	746.5119	PE(16:0p/22:6)	327		418 (436)	mu embryo[39]
747.5	747.5161	PG(16:0/18:1)	255, 281			mu lung[88]
			255, 281		465 (483)	mu embryo[39]
750.5	750.5438	PE(18:0p/20:4)	303		446 (464)	mu brain[164]
		PE(16:0p/22:4)	331		(436)	mu embryo[39]
762.5	762.5286	PS(18:0/16:0)	255, 283	675		mu brain[164]
	762.5068	PE(16:0/22:6)	327,255		434 (452)	mu brain[164]
764.5	764.5229	PE(18:1/20:4)	303, 281		(478)	mu embryo[39]
766.5	766.5387	PE(18:0/20:4)	303, 283		(480)	mu brain[164]
			303, 283			mu lung[39]
770.5	770.5699	PE(20:0/18:2)	279, 508			mu embryo[39]
		PE(18:0/20:2)	283, 307			mu embryo[39]
		PE(18:1/20:1)	281			mu embryo[39]
774.5	774.5432	PE(18:0p/22:6)	327		446 (464)	mu brain[164]
778.5	778.5138	ST(d18:1/16:0)		97, 241		mu ovary[113]
786.5	786.5286	PS(18:1/18:1)	281	699		mu brain[164]
		PS(18:0/18:2)	279, 283	699		mu embryo[39]
788.5	788.5442	PS(18:0/18:1)	281, 283	701		mu brain,[164] mu embryo,[39] mu lung[88]
790.5	790.5381	PE(18:0/22:6)	327, 283		506[d] (524)[e], 462 (480)	hu brain[164,157]
794.5	794.5699	PE(18:0/22:4)	331, 283			hu brain[157]
806.6	806.5451	ST(18:0)		97, 241		mu brain[164]
810.5	810.5286	PS(18:0/20:4)	283, 303	723		mu brain[164]
816.6	816.5755	PS(18:0/20:1)	283, 309	729		mu brain[164]
833.5	833.5181	PI(16:0/18:2)	255, 279	297	553 (571)	mu embryo[39]
834.5	834.5286	PS(18:0/22:6)	283, 327	747		mu brain[164]
837.5	837.5494	PI(18:0/16:0)	283	297	553, 581[d]	mu embryo[39]
857.5	857.5181	PI(16:0/20:4)	255, 303	241	553	mu brain[164]
			255, 303	297	553 (571)	mu embryo[39]
861.5	861.5494	PI(18:0/18:2)	279, 283	297	581 (599)	mu embryo[39]
862.6	862.6077	ST(22:0)		97, 241		mu brain[164]
878.6	878.6078	ST(d18:1/h22:0)		97, 241, 540		rat brain[164]
883.5	883.5337	PI(18:1/20:4)	281, 303	297	579 (597)	mu embryo[39]
885.5	885.5494	PI(18:0/20:4)	283, 303	223, 241	581	mu brain[164]
			283, 303	241	581	mu brain,[8,37] mu ovary[117]
			283, 303	241		mu lung[88]
			283, 303	297	581 (599)	mu embryo[39]
			283, 303	241	581 (599)	rat brain[14]
888.6	888.639	ST(24:1)		97, 241		mu brain,[7,37] rat brain[125,164]
890.6	890.6395	ST(24:0)		97, 241		rat brain[164]
904.6	904.6188	ST(d18:1/h24:1)		97, 241, 540		rat brain[8,164]
906.6	906.6345	ST(d18:1/h24:0)		97, 241, 540		rat brain[14,164]
909.5	909.5488	PI(18:0/22:6)	283, 327	297	581 (599)	mu embryo[39]

[a] Abbreviations: mu, mouse; hu, human. [b] Experimentally measured. [c] Calculated. [d] Loss of R_1COOH. [e] Loss of $R_1CH_2C{=}O$.

dx.doi.org/10.1021/cr200280p |*Chem. Rev.* 2011, 111, 6491–6512

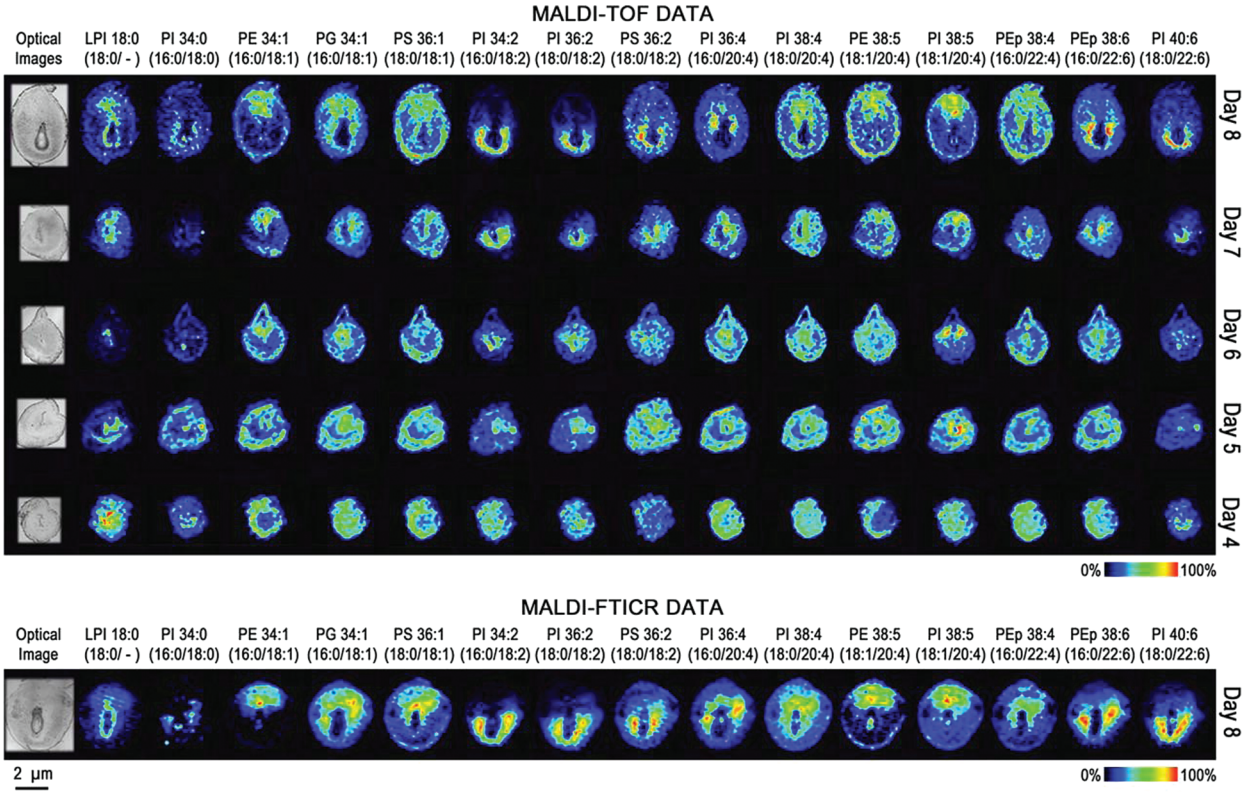

Figure 5. Molecular images of PE, PEp, PI, lysophosphatidylinositol (LPI), PS, and PG on days 4−8 of implantation. MALDI-TOF images (top) and MALDI-FT-ICR images (bottom) of implantation sites are located to the right of their respective optical images. Each column represents a unique phospholipid $[M\text{-}H]^-$, and each row represents a different day of pregnancy. Each image is orientated so the M pole is at the top and the AM pole is at the bottom. Reprinted with permission from ref 39. Copyright 2009 The American Society for Biochemistry and Molecular Biology.

The distribution of PI lipids in pulmonary tissue was also examined using MALDI IMS of the mouse lung.[88] The MALDI images indicated that arachidonate-containing PI lipids, which were identified by the presence of the arachidonic acid carboxylate ion in the CID spectrum as well as the PI-specific product ion at m/z 241, were particularly abundant at the edges of airways when compared to signal intensity in the parenchyma (Figure 6A). This distribution of arachidonate-containing PI lipids was similar to those of the arachidonate-containing PE lipids, and one implication of this lipid localization is that these lipids may be the precursors of eicosanoids during lung inflammation.

4.5. Other Glycerophospholipids

Other classes of phospholipids such as PA, PG, and CL are found in most cells, albeit in lower abundance compared to PC, PE, PI, and PS. PG lipids are present at low levels (1−2%) in most animal tissues and can serve as the precursor of cardiolipin found in mitochondrial membranes. However, PG is uniquely enriched in the lung and constitutes ∼10% of the total phospholipid content in secreted surfactant[89] and is thought to help in the absorption and spreading of surfactant into a functional monolayer.[90] Recently, Voelker and co-workers demonstrated that PG(16:0/18:1) has antiviral properties when instilled into respiratory syncytial virus (RSV)-infected lungs.[91] CL is a phospholipid synthesized from phosphatidylglycerol that contains three glycerol moieties in its backbone and four acyl chains,[92] which is unique among phospholipids. PA is a lipid that constitutes only ∼1% of the total phospholipids in membranes[71] and is an important intermediate for the synthesis of membrane phospholipids. In addition, PA has been implicated in various cellular processes including signal transduction, membrane trafficking, secretion, respiratory burst, and cytoskeletal rearrangement.[93] PG, CL, and PA generate abundant negative ions due to their acidic nature. Each one of these lipids is biologically important, but few studies of MALDI IMS have been reported due to their low abundance. The negative ions $[M\text{-}H]^-$ that have been identified for several of these minor PL molecular species are given in Table 2.

MALDI IMS in the negative ion mode was also employed in the lung studies mentioned above to determine the distribution of PG lipids in pulmonary tissue.[88] The MALDI image of PG(16:0/18:1), which was confirmed by CID, indicated the presence of this lipid uniformly in the lung parenchyma, except for the occurrence of void regions where airways and blood vessels occur (Figure 6B).

Cardiolipin was characterized directly from rat tissues containing high concentrations of mitochondria, such as heart, leg muscle, liver, kidney, and testis.[94] It was found that 2,6-dihydroxyacetophenone was the matrix of choice to observe cardiolipin directly from tissue. The addition of 100 mM CsI along with the matrix increased the sensitivity by driving all of the cardiolipin to a cesium ion adduct. The cardiolipin cesium ion adducts also yielded more informative structural information upon CID. The major cardiolipin imaged by MALDI in the heart, leg muscle, liver, and kidney was $CL(18:2)_4$, whereas the liver and kidney also contained $CL(18:2)_3(18:1)$, but the major cardiolipin present in testis was $CL(16:0)_4$.[94]

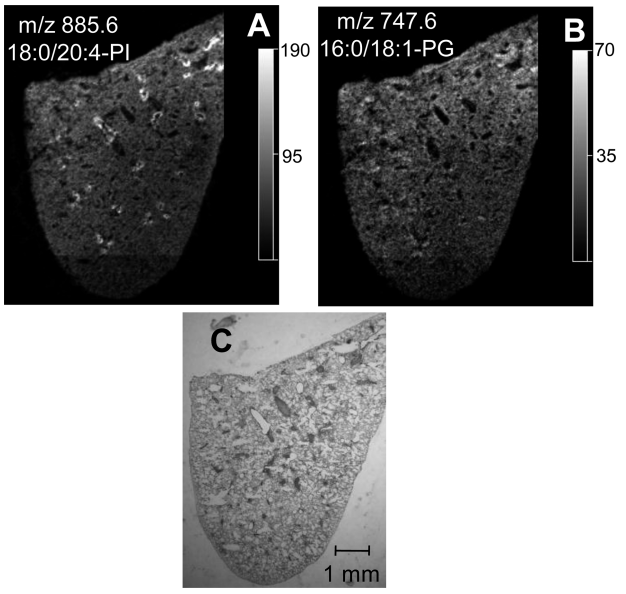

Figure 6. Localization of phosphatidylglycerol and phosphatidylinositol lipids in lung tissue. Extracted negative ion MALDI images of (A) PI(18:0/20:4) at m/z 885.6 and (B) PG(16:0/18:1) at m/z 747.6 from a section a mouse lung. (C) Modified Giemsa stain of the same lung after MALDI imaging. Reprinted with permission from ref 88. Copyright 2011 The American Society for Biochemistry and Molecular Biology.

5. SPHINGOLIPIDS

The biosynthesis of sphingolipids[95] is quite complex but begins with palmitoyl-CoA combining with serine to make 3-ketosphinganine that is converted to sphinganine (Figure 1). Sphinganine can then have its free amino group, N-acylated with another long-chain fatty acyl CoA ester to form a dihydroceramide. This dihydroceramide can be desaturated to form ceramide, containing the long-chain base sphingosine. Diversity in molecular structure arises from differences in the fatty acyl group involved in the N-acylation step as well as initial long-chain base formation. However, the diversity in molecular structure is more complex than that seen for glycerophospholipids due to the presence of hundreds of carbohydrate-based head groups. The primary hydroxyl group of sphingosine can be transformed into quite complex molecular species of glycosphingolipids by conjugation with both simple and complex sugars. There is enormous diversity present in these more complex sphingolipids, and considerable structural challenges exist to define both the carbohydrate and lipid portions of the molecule. The *N*-acyl group also has unusual diversity with some molecular species having an α-hydroxy long-chain fatty acyl group. Tables 1 and 2 list some sphingolipid molecular species that have been identified in imaging studies.

5.1. Ceramide

Ceramides are biosynthetic intermediates of sphingolipids and therefore the central core of sphingolipid metabolism. These lipids are also involved in the regulation of signal transduction processes including cellular apoptosis,[96] cell differentiation,[97] and inflammatory responses.[98] Typically ceramides have long *N*-acyl chains ranging from 16 to 26 carbons in length[99] and would therefore be observed from m/z 538−630. These lipids have been observed as positive ions directly off-tissue[76] and are often dehydrated during the

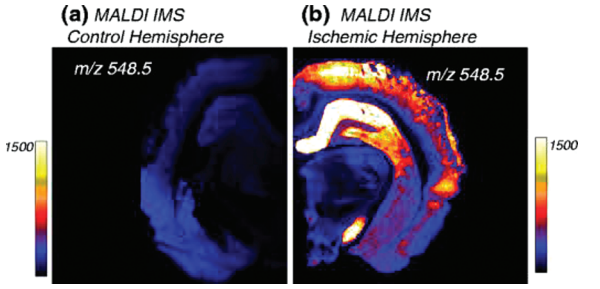

Figure 7. MALDI IMS representing m/z 548.5 ($[M+H-H_2O]^+$, Cer(d18:0/18:1)) in rat brain from (a) single hemisphere of control animal; (b) single hemisphere of animal subjected to bilateral ischemia. Reprinted with permission from ref 76. Copyright 2011 American Society for Mass Spectrometry.

MALDI IMS experiment and observed as $[M+H-H_2O]^+$, which would alter the mass range of observation during MALDI IMS to m/z 520−612. Hankin and co-workers used MALDI IMS to examine the localization of ceramide lipid molecular species in ischemia/reperfusion injured rat brain.[76] Upon ischemia/reperfusion injury, it was found that there was an increase in the abundance of the ion at m/z 548.5 in the ischemic hemisphere localized in the CA1 region of the hippocampus of the injured brain (Figure 7). Collisional activation revealed that this ion was consistent with Cer(d18:1/18:0), which appeared in the MALDI image as a dehydrated product ion $[M+H-H_2O]^+$. It is possible that these dehydrated ceramide ions observed in the MALDI IMS experiment could be derived from a cerebroside, which loses a sugar moiety to form a dehydrated ceramide ion; however, ceramides have been shown previously in other experiments to increase by 150% in the ischemic hippocampus.[100] Even though the formation of ceramides during ischemia/reperfusion injury has been well established, this was the first report of the highly localized nature of these lipids. The colocalization of ceramide production and neuronal cell death in the CA1 region might suggest that sphingomyelin metabolism may have a role in neuronal cell death in the hippocampus during ischemic injury, although these ceramides may arise from de novo biosynthesis or turnover of glycosphingolipids in that area.

5.2. Sphingomyelin

SM functions as a structural component of plasma membranes, and in most mammalian cells the SM content ranges from 5 to 10% of the total phospholipid.[71] However, much higher levels of SM are present in erythrocytes, ocular lenses, and brain.[101] In addition to its structural role, the products of SM metabolism, such as ceramide, sphingosine, sphingosine-1-phosphate, and diacylglycerol, are also involved in cell signaling. These SM-derived products provide SM with a role in cellular functions like apoptosis, aging, and development.[102]

SM lipids contain choline, a quaternary amino group, as a result of phosphocholine transfer from PC to ceramide, which is catalyzed by sphingomyelin synthase.[103] Interestingly there are differences in the MALDI mass spectral behavior of these seemingly similar lipids. An equimolar mixture of SM and PC yields a more intense $[M+H]^+$ from SM when pure molecules are mixed with the matrix before spotting.[104] Yet the typical MALDI IMS (positive ions) of a tissue slice has substantially lower signal for SM relative to the PC molecular species, while analysis of the same brain region by liquid chromatography−tandem

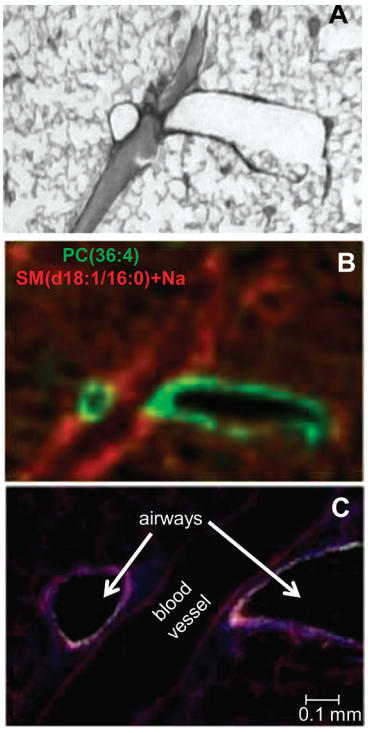

Figure 8. Anatomical structures in the lung were unequivocally identified by dual immunofluorescence and compared to the MALDI images. (A) Enlargement of the boxed part of the modified Giemsa stain of a section of a mouse lung that was inflated and embedded with modified optimal cutting temperature compound. (B) Merged positive ion MALDI image of PC(36:4) (green) and SM(d18:1/16:0)+Na (red). (C) Adjacent tissue section illustrating the localization of airways by acetylated tubulin (ACT, green), blood vessels by thrombomodulin (TM, red), and cell nuclei by DAPI (blue). Reprinted with permission from ref 88. Copyright 2011 The American Society for Biochemistry and Molecular Biology.

mass spectrometry (LC-MS/MS) techniques reveals almost equal abundance of these two lipids.[58] Perhaps this is due to a poorer ability of SM to migrate into the crystal lattice of the matrix as a result of different location within the membrane compartment of cells, or even tighter binding of SM to proteins relative to PC molecules. For example, SM is known to be incorporated into membrane microdomains (often called lipid rafts) along with cholesterol. These microdomains have a high phase-transition temperature, which may place SM in a domain so stable that it poorly mixes with the MALDI matrix. In any event, these observations suggest that caution must be exercised in interpreting absolute abundance of ions across lipid classes (e.g., phospholipids versus sphingolipids). In the study of lung tissue presented above in section 4.4, SM was observed to be associated with blood vessels (Figure 8) rather than pulmonary airways as confirmed by dual immunofluorescence.[88]

5.3. Sulfatides

Sulfoglycosphingolipids are acidic glycosphingolipids that contain a highly anionic sulfate ester moiety and a high proportion of very long chain and α-hydroxy long-chain fatty acyl group attached to the amino nitrogen atom of the ceramide backbone.[105] Sulfated galactosylceramide (sulfatide) and sulfated galactosylalkylacylglycerol (seminolipid) are the two major sulfoglycosphingolipids found in mammals[106] and are derived directly from the sulfation of galactosylceramides catalyzed by galactosylceramide sulfotransferase using 3′-phosphoadenosine-5′-phosphosulfate as the sulfate donor.[105] Sulfatides are abundant in the myelin sheath in the brain,[107] kidney,[108] and islets of Langerhans,[109] whereas seminolipids are found in testis.[110] Additionally, other complex sulfatides, such as lactosylsulfatide, are found in the kidney and are markedly increased in some cancerous tissue.[111,112] Because of the strong acidic character of the sulfate ester, these lipids are observed as negative ions $[M-H]^-$ in MALDI IMS.

MALDI IMS was applied to cancerous ovarian tissue samples to determine the localization of sulfatides, which were found to be elevated in cancerous ovarian tissue compared to normal tissue by LC-MS/MS.[113] Ovarian cancer tissue is composed of many different cell types, including ovarian epithelial carcinoma and nonmalignant stromal tissue. Various sulfatides including ST(d18:1/16:0), ST(d18:1/24:0), and ST(18:1/24:1) were found to be localized to regions of ovarian epithelial carcinoma, in strong contrast with the stromal regions, which were essentially free of sulfatide lipids. The product ions from CID of sulfatide lipids on tissue included m/z 97, the sulfate group, and m/z 241 from release of the sulfated sugar group, which confirmed the identity of these molecular species as sulfatide lipids. MALDI IMS was also used to analyze normal ovarian tissue, which showed that sulfatides were not detectable. These studies indicate that there might be molecular markers, such as ST, that are detectable by MALDI IMS analysis of biopsy samples and allow identification of early tumors that would otherwise be incorrectly scored as "normal" by histologic staining alone. In addition, the MALDI IMS has been applied to determine the localization of complex sulfatides in the kidney[114] and to seminolipids in testis.[115]

5.4. Other Sphingolipids

Glycosphingolipids refer to a broad subclass of sphingolipids where carbohydrate moieties (glucose as glucocerebroside or glucosylceramide, galactose as galactocerebroside or galactosylceramide, lactose as lactosylceramide), singly or multiply, are enzymatically linked to the ceramide backbone (Figure 1). The term "cerebroside" refers generally to monosaccharide forms, while gangliosides are polysaccharides containing glucose, galactose, and one or more sialic acids (*N*-acetyl neuraminic acid). The array of combinations is complex, with the glycosylation taking place intracellularly at the Golgi complex via a series of glycosyltransferases specific for the substrate, linkage, and ordering of the multiple stacked sugar groups.[116] Glycosphingolipids are present in all tissues, with specific forms predominant in specific tissues. For example, galactocerebrosides are more abundant in white matter of brain tissue.[117] The biology of glycosphingolipids is rich, diverse, and specific to molecular structure, leading to a strong interest to study this class of molecule. Galactosylceramides have been implicated in cell membrane signaling related to membrane folding in the myelin formation of Schwann cells,[118] in Gauchers disease,[119] ganglioside GM3 neuronal cell development,[120] and ganglioside GM1 in neuroprotection.[121]

Mass spectrometry has been applied to the study of glycosphingolipids, which yield abundant positive and negative ions.[122,123] Collisional activation of these molecules resulted in the facile, sequential loss of the sugar components. Recent studies using lithium salts mixed into the MALDI matrix[24] or an

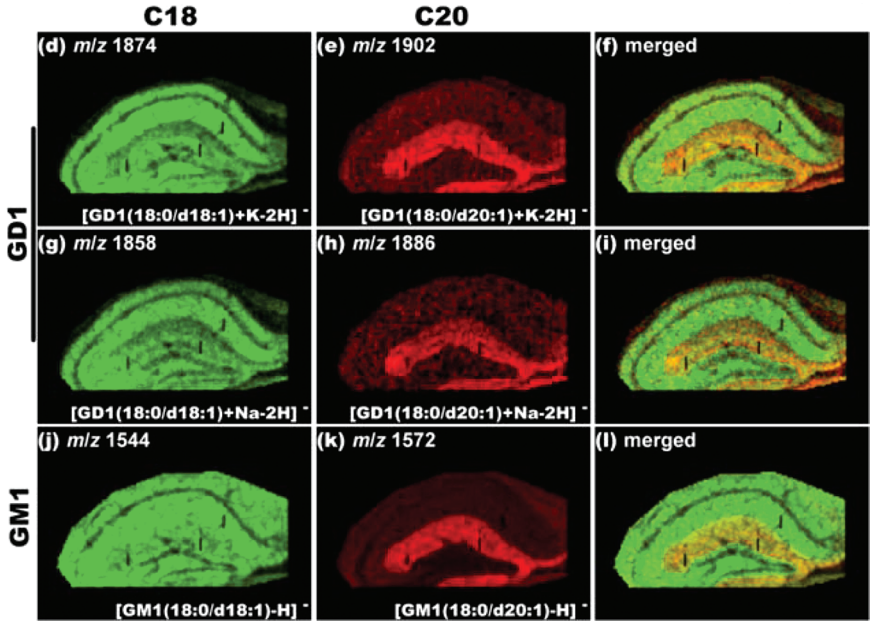

Figure 9. MALDI IMS (negative ion) of gangliosides in mouse hippocampus. The C20 ganglioside (GD1 18:0/d20:1) had greater intensity of the ion m/z 1902 $[M+K-2H]^-$ in the stratum lacunosum moleculare (SLM), relative to the C18 ganglioside (GD1 18:0/d18:1). The structural differences between C20 and C18 gangliosides were due to carbon chain length differences at the membrane-bound ceramide backbone and not at the cytosolic carbohydrate portion of the molecules. This regional distinctiveness was apparent also for the C20 and C18 GM1 gangliosides. This research was originally published as ref 127 as an open access article.

ion trap instrument with MS^3 capability[125] yielded information on the structure of the ceramide backbone. New matrix application methods and instrumentation have extended MALDI IMS techniques to studies of tissue localization of intact glycosphingolipids.[11] Setou and co-workers[127] recently applied MALDI IMS to the study of gangliosides and found regionally distinct ion intensities within the mouse hippocampus for two gangliosides that differed in ceramide carbon number. The C20 ganglioside (GD1 18:0/d20:1) had greater intensity of m/z 1902 $[M+K-2H]^-$ in a specific layer, the stratum lacunosum moleculare, of the mouse hippocampus relative to the C18 ganglioside (GD1 18:0/d18:1) of related structure (Figure 9). Although the functional significance of this localized difference is not known, there was a compelling biological separation of two related sialic acid gangliosides that was uniquely revealed by MALDI IMS.

Several studies have utilized MALDI IMS to characterize components (including glycosphingolipids) developed from thin-layer chromatography (TLC) separation of tissue extracts. This invokes a sensitive and inexpensive method for study of complex lipid mixtures, including multiple subclasses of the glycosphingolipid family.[128−130]

6. NEUTRAL LIPIDS (GLYCEROLIPIDS AND STEROLS)

Neutral lipids are composed of both sterols and glycerolipids, which have very different biosynthetic origins. However, these two classes have similar physical−chemical properties in that they are quite hydrophobic, uncharged, and apolar to slightly polar molecules that must be ionized by the MALDI process to be observed as ions in MALDI IMS studies. The MALDI ions typically observed are $[M+Na]^+$ or $[M+K]^+$, where charging of the neutral TAG by the alkali metal ion during MALDI is a consequence of the presence of alkali metal salts in the biological tissue. It has been suggested that $[M+H]^+$ ion species from TAGs are sufficiently unstable that they decompose too rapidly to be observed.[132,133] Investigators have also added Li^+-salts to promote ionization as the $[M+Li]^+$, which has favorable CID behavior.[135] Subclasses of glycerolipids (GLs) include triacylglycerols (TAGs), diacylglycerols (DAGs), and monoacylglycerols (MAGs). Unambiguous identification of DAGs and MAGs may be compromised in MALDI IMS because prompt ion fragmentation of TAGs[132,133] and phospholipids[132] yield DAG-like ions $(DAG-H_2O+H)^+$, and DAGs and lysophospholipids[132] produce MAG product ions $(MAG-H_2O+H)^+$. There is a dearth of mass spectral information available in the literature concerning the behavior of TAG molecular species during MALDI ionization and subsequent CID of MALDI molecular ion species. This makes it very difficult to assign precise structural details about specific regioisomers because few synthetic standards are available with sufficient diversity in structure (chain length, unsaturation, and esterification position on the glycerol backbone) to probe the ion chemistry of alkali metal adduct ion decomposition. However, it is possible to determine those fatty acyl groups (but not position) that make up the triester moieties of TAGs by CID of the $[M+\text{alkali metal}]^+$ adduct. Although the CID of pure TAG synthetic molecules as the lithiated salt (generated by electrospray ionization) have been shown to yield less abundant product ions corresponding to the loss of the *sn*-2 acyl group as a free acid compared to the signal from loss of the *sn*-1/*sn*-3 acyl chains,[135] there has been at least one paper in the literature to suggest that the sodiated adducts of TAGs do not behave this way.[132] A further complication is that molecular ions from TAGs present in a biological tissue may be composed of several isobaric molecular species[136] that would lead to more than three RCOOH losses from the CID of $[M+Na]^+$. Clearly more work is needed

dx.doi.org/10.1021/cr200280p |*Chem. Rev.* 2011, 111, 6491–6512

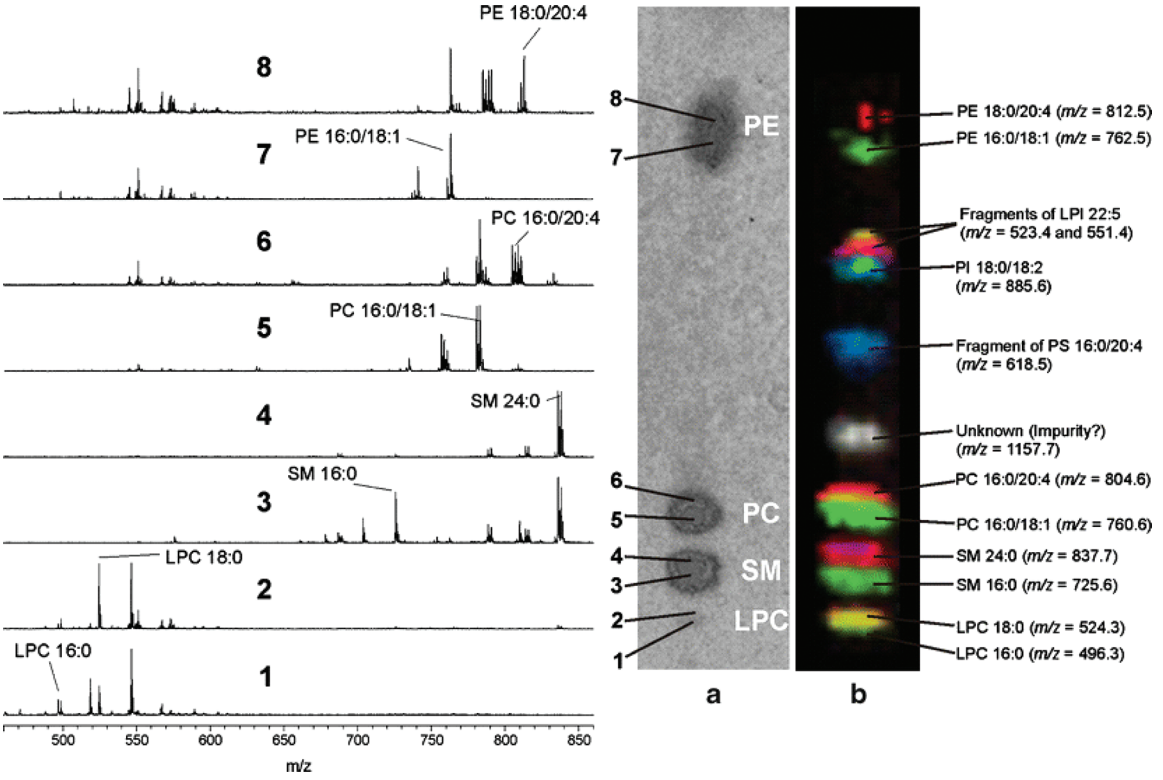

Figure 10. Photographic image of a typical HP-TLC plate of an organic erythrocyte extract (a) and the corresponding MALDI image (b). Mass spectra (left) were recorded from spots subsequent to primuline staining. Only the most intense peaks showing a significant position dependence are annotated in the mass spectra. In the MALDI image recorded subsequent to automatic matrix application, additional classes of phospholipids (e.g., PI) were detected that were not detectable by primuline staining. The structure corresponding to m/z = 1157.7 could not be yet assigned. Reprinted with permission from ref 140. Copyright 2008 Springer.

to study the MALDI-mass spectral behavior of these neutral lipids and the structural parameters that influence the CID process.

Images of the species TAG(52:3)+Na^+ (m/z 879.72, containing 16:0, 18:2, and 18:1 fatty acyl groups), TAG(52:2)+Na^+ (m/z 881.74, containing 16:0, 18:1, and 18:1 fatty acyl groups), and TAG(54:4)+K^+ (m/z 921.74, containing 16:0, 20:3, and 18:1 fatty acyl groups) have been observed around brown adipose tissue in mouse embryos.[137] In an image from mouse kidney, the signal for m/z 879.7 was found to yield abundant collisional activation product ions at m/z 623.5, 597.5, and 575.5, but was likely misidentified and reported to be a $[M+H]^+$.[37] Upon a more detailed examination, this TAG molecular ion and the CID spectra were found to be more consistent with an $[M+Na]^+$ containing 16:0, 18:2, and 18:1 fatty acyl groups. The product ion corresponding to the loss of 304 Da from the molecular ion (m/z 575.5) was more likely due to the loss of $C_{18}H_{33}O_2Na$ from the $[M+Na]^+$ by a slightly different mechanism than that responsible for the loss of the free carboxylic acid (RCOOH). This TAG molecular species seemed to be present in the perirenal fat tissue around the kidney.[37]

A third IMS study of rat kidney indicated the presence of TAG(54:3) and TAG(52:3) as potassiated adduct ions.[25] MS/MS confirmation of the TAG composition was obtained by formation of lithium adduct ions.[25] TAG(54:3) has also been identified in an image of human skin; the identification of this species was based on an accurate mass determination for the sodiated ion (m/z 907.7731).[139]

The most abundant neutral lipid present in cellular membranes is cholesterol. However, only a few MALDI IMS images of this neutral lipid have been reported as the ion at m/z 369.3.[25,37] Further characterization of this ion has not been reported by CID studies. Because cholesterol yields this dehydrated molecular ion fairly readily during MALDI and the reported images have been rather noninformative, this neutral lipid has not received much attention by those performing MALDI IMS studies.

7. OTHER LIPID APPLICATIONS

There are a number of reports in which MALDI IMS of lipids has been used in studies of nontissue samples. This is a growing general application, and three examples will be illustrated.

7.1. Thin-Layer Chromatography

One interesting application of MALDI IMS was in combination with thin-layer chromatography (TLC), which has enabled sensitive and detailed analyses of lipids. TLC is routinely used for lipid separation and is usually followed by mass spectrometry detection of lipid compounds after extraction of the lipids from the TLC plate; however, this assay is time-consuming and analyte recovery can be poor. One way to easily and quickly obtain information about the lipid molecular species present on a TLC plate after a chromatographic separation is to use MALDI IMS. This technique has been used to analyze the phospholipids present in erythrocytes.[140] Only three lipid classes (PC, SM, and PE) were visualized with

dx.doi.org/10.1021/cr200280p |*Chem. Rev.* 2011, 111, 6491–6512

primuline stain (Figure 10a), whereas with the TLC-MALDI-IMS technique, 6 different classes of lipids (PG, PE, PI, PS, PC, and SM) (Figure 10b) were detected. The image in the figure clearly shows the superior sensitivity of MALDI IMS compared to staining. Additionally, TLC-MALDI-IMS enabled more detailed information about the lipids present in each spot of the TLC plate to be determined (Figure 10 mass spectra 1−8) compared to staining alone. Another method called TLC-blot-MALDI-IMS has also been developed where lipids were heat-transferred directly from the TLC plate to a polyvinylidene difluoride membrane.[141−143] The membrane was then mounted to a MALDI plate, coated with matrix, and analyzed by MALDI IMS. This method has been explored because the sensitivity, mass resolution, and background interference in the mass spectrometry data from these membranes has been reported to be superior to that obtained directly from TLC plates.[142] One application of this TLC-blot-MALDI-IMS method is in the comparison of the ganglioside compositions of normal and Alzheimer's disease patients.[128] It was revealed that a change in ganglioside composition was observed in the hippocampus gray matter of Alzheimer's disease patients. It is clear that the application of MALDI IMS to detect lipids separated on TLC plates is much more sensitive and provides more information than traditional staining techniques.

7.2. Forensic Analysis

Another application of MALDI IMS of lipids has been in the field of forensic science. In one application of MALDI IMS, the construction of latent fingermarks using endogenous lipid ions was achieved.[144] This experimental methodology was developed using the protonated oleic acid ion at m/z 283.2, and the authors point out that the matrix ion signals of α-cyano-4-hydroxycinnamic acid did not interfere with the detection of this low mass analyte ion, which is quite surprising because matrix background ions often mask low mass analyte signals in MALDI studies. In addition to oleic acid, the distribution of other endogenous lipids, such as cholesterol, stearic acid, and DAGs, produced fingermark images (Figure 11). Aged fingermark studies were also completed, and it was found that the intensity of the lipid ion signal decreases with both time and temperature. It was suggested by the authors that this technology might be useful to date latent fingermarks and place a subject at the scene of a crime at a particular time.

7.3. Diagnosis

MALDI IMS of proteins is currently used as a diagnostic tool in a clinical setting. For example, Caprioli and co-workers have successfully applied MALDI IMS to predict responsiveness to neoadjuvant taxane therapy and radiation in breast cancer[145] and determination of molecular tumor margins in clear cell renal cell carcinoma.[146] These studies have provided insight into disease that is not obtainable by standard histological techniques. However, not many reports have been published on the use of MALDI IMS of phospholipids as a diagnostic tool.

Previous studies have suggested that cancerous tissue contains elevated amounts of total phospholipid and altered composition of the membranes of metastatic cancer cells and nonmetastatic cells.[147] There have been several reports that glycosphingolipids, sphingolipids, and glycerophosphocholine lipids are increased in various types of cancer. For example, the presence of STs is associated with a poor outcome in renal,[148] lung,[111] and ovarian cancers.[149] Additionally, brain, colon, lung, and prostate tumors show elevated levels of PCs, with the highest levels associated with the most aggressive tumors.

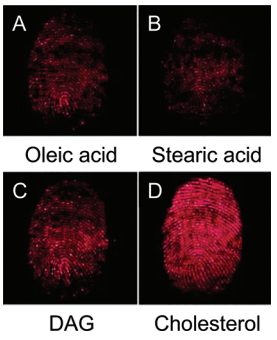

Figure 11. MALDI-MSI analysis of an ungroomed, fresh fingermark. (A) Fingermark MS image reconstructed from the ion signal at m/z 283 (oleic acid), (B) m/z 285, (stearic acid), (C) m/z 669.6 (diacylglycerol), and (D) m/z 369 (cholesterol). Modified from the original figure. Reprinted with permission from ref 144. Copyright 2009 John Wiley.

MALDI IMS has been applied to cancerous tissues to determine the spatial distribution of lipids and determine if lipids can be markers for the detection and diagnosis of cancer. In one study of human colon cancer liver metastases, the MALDI image of m/z 725.6, SM(d18:1/16:0)+Na^+, indicated that this SM was present in the cancerous tissue and the stroma area but not present in the normal liver tissue.[18] This MALDI image correlated with previous work that demonstrated that SMs were increased in cancerous colonocytes. MALDI IMS of myxoid liposacroma revealed differences between low- and high-grade tumors.[150] It was found that PCs were present in both low- and high-grade tumors but yielded higher intensity signals in the high-grade tumors. The higher levels of PCs were consistent with the higher cellularity of high-grade tumors and are consistent with previous NMR studies that found increased PC lipids in high-grade myxoid liposarcoma tumors. Additionally, low-grade myxoid liposarcoma tumors showed an increase in TAGs compared to the high-grade tumors. This study clearly showed a correlation between lipid composition with the histology and grade of a myxoid liposarcoma tumor. In section 5.3, an elegant study on sulfatide localization in ovarian cancer was described.[113] These studies implicated the use of MALDI IMS for specific lipid molecules in biopsy samples to facilitate early identification of cancer.

8. CONCLUSION

Lipid biochemistry occurring within living tissues is complex, and a multitude of distinct families of lipids are synthesized by cells, each with very different chemical structures and diverse biological properties. Mass spectrometry has emerged as an important technique for the detection as well as the identification of lipid structures, with MALDI IMS becoming a creative tool to specify location of lipids in tissue slices. The spatial resolution of MALDI IMS limits applications to the tissue level, but rapid developments in technology suggest that subcellular studies of lipid biochemistry are just around the corner. Current studies of lipids with MALDI IMS show distinct localization of specific lipids of multiple classes related to tissue region or cell type. These images underline the local accumulation of specific lipids and imply that distinct

biochemical events take place in certain tissue regions. The intensity differences observed for specific ions support meaningful differences in amounts of lipids within limitations of recognized complexity of tissue matrices and chemical and instrumental variables. Future studies to connect exact biochemical events to changes in lipid accumulation and cellular relevance will likely be forthcoming.

AUTHOR INFORMATION

Corresponding Author

*Tel.: 303-724-3352. Fax: 303-724-3357. E-mail: robert.murphy@ucdenver.edu.

Author Contributions

§Both authors contributed equally to this review.

BIOGRAPHIES

Karin A. Zemski Berry received her B.S. in Chemistry from Shippensburg University in 1996 and her Ph.D. in Chemistry from The Pennsylvania State University in 2001. She did her postdoctoral training in Robert Murphy's lab at National Jewish Health and is now a Senior Research Associate in Robert Murphy's lab at University of Colorado Denver. Her current research interests focus mainly on oxidized lipids in diseased and damaged lung tissue and the application of MALDI imaging to biologically relevant lung tissue samples.

Joseph A. Hankin received a B.A. in Special Education from Northeastern Illinois University (1982) and worked for several years in a program for special needs children before returning to school for a second B.A. in Biology (1989) and M.S. in Chemistry (1992) from University of Colorado Denver. He completed his Ph.D. (1995) in organic chemistry at the University of Colorado at Boulder. After postdoctoral work at National Jewish Health in Denver with Robert Murphy, he remained with the Murphy Lab to continue studies related to lipid biochemistry. Recent research interests have involved the application of imaging mass spectrometry to studies of lipids in tissue inflammation models.

Robert Barkley received a B.A in chemistry from St. Olaf College in 1970 and Ph.D. in inorganic chemistry from the University of Colorado at Boulder in 1976. His interests in the application of mass spectrometry for chemical analysis have ranged from the characterization of inorganic molecular species and studies of trace organic compounds in water and air, to lipids in biological systems, including intact tissues.

Jeffrey M. Spraggins received his B.A. in Chemistry from the College of Wooster and his Ph.D. in Analytical Chemistry from the University of Delaware (2009), where he studied gas-phase fragmentation mechanisms of modified biomolecules in addition to developing new Problem-Based Learning activities to help undergraduate and high school students understand science. Currently, Dr. Spraggins is a Postdoctoral Research Fellow with the National Research Resource in Imaging Mass Spectrometry at Vanderbilt University. His research interests include developing new mass spectrometric technologies to enhance lipid imaging experiments. Specifically, he is working on expanding the application of FT-ICR MS in the field of imaging mass spectrometry and is involved in developing next-generation high performance MALDI-TOF instrumentation.

Richard M. Caprioli is Professor of Biochemistry, Chemistry, Medicine and Pharmacology at Vanderbilt University. Dr. Caprioli received his B.S. in 1965 from Columbia University in New York, NY, and his Ph.D. in 1969 in Biochemistry, also at Columbia University. Dr. Caprioli has been President of ASMS; has been Editor-in-Chief of the *Journal of Mass Spectrometry* since 1990; and is currently serving a 3-year term on the Board of Directors of HUPO. Dr. Caprioli received the Thomson Medal Award from the International Mass Spectrometry Society in 2003, the Field and Franklin Award from the American Chemical Society in April, 2006, and the HUPO Distinguished Achievement Award in Proteomic Sciences for 2010. Professor Caprioli's general research interests lie in discovery of temporal and spatial processes in biological systems using mass spectrometry. Recent work involves the development of Imaging Mass Spectrometry, a technology whereby molecular images of peptides, proteins, drugs, and other compounds are localized in tissue sections with molecular weight specificity. He has published over 300 peer-reviewed articles.

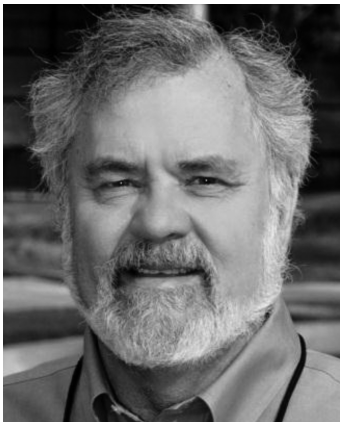

Robert C. Murphy received his B.S. in Chemistry from Mount Union College (1966) and his Ph.D. in Chemistry from Massachusetts Institute of Technology (1970). After postdoctoral studies at Harvard Medical School, he joined the faculty in Pharmacology at the University of Colorado Health Science Center in 1971. He was a member of the faculty of National Jewish Health from 1989 to 2004 when he returned to the University of Colorado Denver and is now a University Distinguished Professor. His research interests center on the biochemistry and pharmacology of bioactive lipid mediators including leukotrienes, platelet activating factor, metabolites of arachidonic acid, and oxidized phospholipids. In his research studies, mass spectrometric approaches are featured to study lipid biochemistry. Dr. Murphy has been president of the American Society for Mass Spectrometry and served on the Executive Board for 6 years. He is the author of over 400 publications.

ACKNOWLEDGMENT

This work was supported in part by grants from the National Institutes of Health: HL034303 (R.C.M.), GM069338 (R.C.M.), RRR031461 (R.M.C.), and GM058008 (R.M.C.).

REFERENCES

(1) Fahy, E.; Subramaniam, S.; Brown, H. A.; Glass, C. K.; Merrill, A. H., Jr.; Murphy, R. C.; Raetz, C. R. H.; Russell, D. W.; Seyama, Y.; Shaw, W.; Shimizu, T.; Spener, F.; van Meer, G.; VanNieuwenhze, M. S.; White, S. H.; Witztum, J. L.; Dennis, E. A. *J. Lipid Res.* **2005**, *46*, 839.
(2) Touboul, D.; Brunelle, A.; Laprevote, O. *Biochimie* **2011**, *93*, 113.
(3) Chughtai, K.; Heeren, R. M. *Chem. Rev.* **2010**, *110*, 3237.
(4) Stauber, J.; MacAleese, L.; Franck, J.; Claude, E.; Snel, M.; Kaletas, B. K.; Wiel, I. M.; Wisztorski, M.; Fournier, I.; Heeren, R. M. *J. Am. Soc. Mass Spectrom.* **2010**, *21*, 338.
(5) Jackson, S. N.; Ugarov, M.; Egan, T.; Post, J. D.; Langlais, D.; Albert, S. J.; Woods, A. S. *J. Mass Spectrom.* **2007**, *42*, 1093.
(6) Caprioli, R. M.; Farmer, T. B.; Gile, J. *Anal. Chem.* **1997**, *69*, 4751.
(7) Garrett, T. J.; Prieto Conaway, M. C.; Kovtoun, V.; Bui, H.; Izgarian, N.; Stafford, G.; Yost, R. A. *Int. J. Mass Spectrom.* **2007**, *260*, 166.
(8) Shimma, S.; Sugiura, Y.; Hayasaka, T.; Zaima, N.; Matsumoto, M.; Setou, M. *Anal. Chem.* **2008**, *80*, 878.
(9) Altelaar, A. F.; Klinkert, I.; Jalink, K.; de Lange, R. P.; Adan, R. A.; Heeren, R. M.; Piersma, S. R. *Anal. Chem.* **2006**, *78*, 734.
(10) Astigarraga, E.; Barreda-Gomez, G.; Lombardero, L.; Fresnedo, O.; Castano, F.; Giralt, M. T.; Ochoa, B.; Rodriguez-Puertas, R.; Fernandez, J. A. *Anal. Chem.* **2008**, *80*, 9105.
(11) Chan, K.; Lanthier, P.; Liu, X.; Sandhu, J. K.; Stanimirovic, D.; Li, J. *Anal. Chim. Acta* **2009**, *639*, 57.
(12) Jun, J. H.; Song, Z.; Liu, Z.; Nikolau, B. J.; Yeung, E. S.; Lee, Y. J. *Anal. Chem.* **2010**, *82*, 3255.
(13) Meriaux, C.; Franck, J.; Wisztorski, M.; Salzet, M.; Fournier, I. *J. Proteomics* **2010**, *73*, 1204.
(14) Shanta, S. R.; Zhou, L. H.; Park, Y. S.; Kim, Y. H.; Kim, Y.; Kim, K. P. *Anal. Chem.* **2011**, *83*, 1252.
(15) Shrivas, K.; Hayasaka, T.; Goto-Inoue, N.; Sugiura, Y.; Zaima, N.; Setou, M. *Anal. Chem.* **2010**, *82*, 8800.
(16) Cha, S.; Yeung, E. S. *Anal. Chem.* **2007**, *79*, 2373.
(17) Bouschen, W.; Schulz, O.; Eikel, D.; Spengler, B. *Rapid Commun. Mass Spectrom.* **2010**, *24*, 355.
(18) Shimma, S.; Sugiura, Y.; Hayasaka, T.; Hoshikawa, Y.; Noda, T.; Setou, M. *J. Chromatogr., B* **2007**, *855*, 98.
(19) Franck, J.; Arafah, K.; Barnes, A.; Wisztorski, M.; Salzet, M.; Fournier, I. *Anal. Chem.* **2009**, *81*, 8193.
(20) Grove, K. J.; Frappier, S. L.; Caprioli, R. M. *J. Am. Soc. Mass Spectrom.* **2011**, *22*, 192.
(21) Baluya, D. L.; Garrett, T. J.; Yost, R. A. *Anal. Chem.* **2007**, *79*, 6862.
(22) Hankin, J. A.; Barkley, R. M.; Murphy, R. C. *J. Am. Soc. Mass Spectrom.* **2007**, *18*, 1646.
(23) Puolitaival, S. M.; Burnum, K. E.; Cornett, D. S.; Caprioli, R. M. *J. Am. Soc. Mass Spectrom.* **2008**, *19*, 882.
(24) Cerruti, C. D.; Touboul, D.; Guerineau, V.; Petit, V. W.; Laprevote, O.; Brunelle, A. *Anal. Bioanal. Chem.* **2011**, *401*, 75.
(25) Sugiura, Y.; Setou, M. *Rapid Commun. Mass Spectrom.* **2009**, *23*, 3269.
(26) Fernandez, J. A.; Ochoa, B.; Fresnedo, O.; Giralt, M. T.; Rodriguez-Puertas, R. *Anal. Bioanal. Chem.* **2011**, *401*, 29.

(27) Goto-Inoue, N.; Hayasaka, T.; Zaima, N.; Setou, M. *Biochim. Biophys. Acta* DOI: 10.1016/j.bbalip.2011.03.004. Available online: Mar 24, 2011; http://www.sciencedirect.com/science/article/pii/S1388198111000-345 (accessed Aug 23, 2011).
(28) Petkovic, M.; Schiller, J.; Mueller, M.; Benard, S.; Reichl, S.; Arnold, K.; Arnhold, J. *Anal. Biochem.* **2001**, *289*, 202.
(29) Schiller, J.; Suss, R.; Petkovic, M.; Zschornig, O.; Arnold, K. *Anal. Biochem.* **2002**, *309*, 311.
(30) Russell, D. H.; Edmondson, R. D. *J. Mass Spectrom.* **1997**, *32*, 263.
(31) Landgraf, R. R.; Prieto Conaway, M. C.; Garrett, T. J.; Stacpoole, P. W.; Yost, R. A. *Anal. Chem.* **2009**, *81*, 8488.
(32) Marshall, A. G.; Hendrickson, C. L.; Jackson, G. S. *Mass Spectrom. Rev.* **1998**, *17*, 1.
(33) Murphy, R. C.; Axelsen, P. H. *Mass Spectrom. Rev.* **2011**, *30*, 579.
(34) Hsu, F. F.; Turk, J. *J. Chromatogr., B* **2009**, *877*, 2673.
(35) Gunstone, F. D.; Herslöf, B. G. *A Lipid Glossary*; The Oily Press LTD: Dundee, Scotland, 1992.
(36) Ho, Y. P.; Huang, P. C. *Rapid Commun. Mass Spectrom.* **2002**, *16*, 1582.
(37) Murphy, R. C.; Hankin, J. A.; Barkley, R. M. *J. Lipid Res.* **2009**, *50*, S317.
(38) Jackson, S. N.; Wang, H. Y.; Woods, A. S. *J. Am. Soc. Mass Spectrom.* **2005**, *16*, 2052.
(39) Burnum, K. E.; Cornett, D. S.; Puolitaival, S. M.; Milne, S. B.; Myers, D. S.; Tranguch, S.; Brown, H. A.; Dey, S. K.; Caprioli, R. M. *J. Lipid Res.* **2009**, *50*, 2290.
(40) Hsu, F. F.; Bohrer, A.; Turk, J. *J. Am. Soc. Mass Spectrom.* **1998**, *9*, 516.
(41) Han, X.; Gross, R. W. *J. Am. Soc. Mass Spectrom.* **1995**, *6*, 1202.
(42) Simoes, C.; Simoes, V.; Reis, A.; Domingues, P.; Domingues, M. R. *Rapid Commun. Mass Spectrom.* **2008**, *22*, 3238.
(43) Stubiger, G.; Pittenauer, E.; Allmaier, G. *Anal. Chem.* **2008**, *80*, 1664.
(44) Pulfer, M.; Murphy, R. C. *Mass Spectrom. Rev.* **2003**, *22*, 332.
(45) Han, X.; Gross, R. W. *Proc. Natl. Acad. Sci. U.S.A.* **1994**, *91*, 10635.
(46) Hsu, F. F.; Turk, J. *J. Am. Soc. Mass Spectrom.* **2000**, *11*, 986.
(47) Hsu, F. F.; Turk, J. *J. Am. Soc. Mass Spectrom.* **2005**, *16*, 1510.
(48) Herrera, L. C.; Potvin, M. A.; Melanson, J. E. *Rapid Commun. Mass Spectrom.* **2010**, *24*, 2745.
(49) Fillet, M.; Van Heugen, J. C.; Servais, A. C.; De, G. J.; Crommen, J. *J. Chromatogr., A* **2002**, *949*, 225.
(50) Hsu, F. F.; Turk, J. *J. Am. Soc. Mass Spectrom.* **2004**, *15*, 536.
(51) Sparagna, G. C.; Johnson, C. A.; McCune, S. A.; Moore, R. L.; Murphy, R. C. *J. Lipid Res.* **2005**, *46*, 1196.
(52) Hsu, F. F.; Turk, J.; Rhoades, E. R.; Russell, D. G.; Shi, Y.; Groisman, E. A. *J. Am. Soc. Mass Spectrom.* **2005**, *16*, 491.
(53) Pariza, M. W.; Park, Y.; Cook, M. E. *Prog. Lipid Res.* **2001**, *40*, 283.
(54) Drake, D. R.; Brogden, K. A.; Dawson, D. V.; Wertz, P. W. *J. Lipid Res.* **2008**, *49*, 4.
(55) Thomas, M. C.; Mitchell, T. W.; Harman, D. G.; Deeley, J. M.; Nealon, J. R.; Blanksby, S. J. *Anal. Chem.* **2008**, *80*, 303.
(56) Castro-Perez, J.; Roddy, T. P.; Nibbering, N. M. M.; Shah, V.; McLaren, D. G.; Previs., S.; Attygalle, A. B.; Herath, K.; Chen, Z.; Wang, S.-P.; Mitnaul, L.; Hubbard, B. K.; Vreeken, R. J.; Johns, D. G.; Hankemeier, T. *J. Am. Soc. Mass Spectrom.* **2011**, *22*, 1552.
(57) Guo, Z.; He, L. *Anal. Bioanal. Chem.* **2007**, *387*, 1939.
(58) Hankin, J. A.; Murphy, R. C. *Anal. Chem.* **2010**, *82*, 8476.
(59) Fadeel, B.; Xue, D. *Crit Rev. Biochem. Mol. Biol.* **2009**, *44*, 264.
(60) Gibellini, F.; Smith, T. K. *IUBMB Life* **2010**, *62*, 414.
(61) Voelker, D. R. *Biochim. Biophys. Acta* **2000**, *1486*, 97.
(62) Farooqui, A. A.; Ong, W. Y.; Horrocks, L. A. *Adv. Exp. Med. Biol.* **2003**, *544*, 335.
(63) Carman, G. M.; Kersting, M. C. *Biochem. Cell Biol.* **2004**, *82*, 62.
(64) Vance, J. E.; Vance, D. E. *Biochem. Cell Biol.* **2004**, *82*, 113.
(65) Shindou, H.; Shimizu, T. *J. Biol. Chem.* **2009**, *284*, 1.
(66) Ghosh, M.; Tucker, D. E.; Burchett, S. A.; Leslie, C. C. *Prog. Lipid Res.* **2006**, *45*, 487.
(67) Gijon, M. A.; Riekhof, W. R.; Zarini, S.; Murphy, R. C.; Voelker, D. R. *J. Biol. Chem.* **2008**, *283*, 30235.
(68) Sartain, M. J.; Dick, D. L.; Rithner, C. D.; Crick, D. C.; Belisle, J. T. *J. Lipid Res.* **2011**, *52*, 861.
(69) Catala, A. *Chem. Phys. Lipids* **2009**, *157*, 1.
(70) Basu, S. *Prostaglandins, Leukotrienes Essent. Fatty Acids* **2010**, *82*, 219.
(71) Vance, J. E.; Steenbergen, R. *Prog. Lipid Res.* **2005**, *44*, 207.
(72) Billah, M. M.; Anthes, J. C. *Biochem. J.* **1990**, *269*, 281.
(73) Mueller, H. W.; O'Flaherty, J. T.; Wykle, R. L. *Lipids* **1982**, *17*, 72.
(74) Ojima-Uchiyama, A.; Masuzawa, Y.; Sugiura, T.; Waku, K.; Saito, H.; Yui, Y.; Tomioka, H. *Lipids* **1988**, *23*, 815.
(75) Arthur, G.; Mock, T.; Zaborniak, C.; Choy, P. C. *Lipids* **1985**, *20*, 693.
(76) Hankin, J. A.; Farias, S.; Barkley, R. M.; Heidenreich, K.; Frey, L. C.; Hamazaki, K.; Kim, H.-Y.; Murphy, R. C. *J. Am. Soc. Mass Spectrom.* **2011**, *22*, 1014.
(77) Verkleij, A. J.; Leunissen-Bijvelt, J.; de, K. B.; Hope, M.; Cullis, P. R. *Ciba Found. Symp.* **1984**, *103*, 45.
(78) Jin, X. H.; Okamoto, Y.; Morishita, J.; Tsuboi, K.; Tonai, T.; Ueda, N. *J. Biol. Chem.* **2007**, *282*, 3614.
(79) Bacot, S.; Bernoud-Hubac, N.; Chantegrel, B.; Deshayes, C.; Doutheau, A.; Ponsin, G.; Lagarde, M.; Guichardant, M. *J. Lipid Res.* **2007**, *48*, 816.
(80) Miyazawa, T.; Nakagawa, K.; Shimasaki, S.; Nagai, R. *Amino Acids* DOI: 10.1007/s00726-010-0772-3. Published online: Oct 19, 2010; http://dx.doi.org/10.1007/s00726-010-0772-3 (accessed Aug 23, 2011).
(81) Sparrow, J. R.; Wu, Y.; Kim, C. Y.; Zhou, J. *J. Lipid Res.* **2010**, *51*, 247.
(82) Bratton, D. L.; Henson, P. M. *Curr. Biol.* **2008**, *18*, R76.
(83) Nishizuka, Y. *Science* **1992**, *258*, 607.
(84) Hicks, A. M.; DeLong, C. J.; Thomas, M. J.; Samuel, M.; Cui, Z. *Biochim. Biophys. Acta* **2006**, *1761*, 1022.
(85) DiPaolo, G.; DeCamilli, P. *Nature* **2006**, *443*, 651.
(86) Holub, B. J.; Kuksis, A.; Thompson, W. *J. Lipid Res.* **1970**, *11*, 558.
(87) Vanhaesebroeck, B.; Leevers, S. J.; Ahmadi, K.; Timms, J.; Katso, R.; Driscoll, P. C.; Woscholski, R.; Parker, P. J.; Waterfield, M. D. *Annu. Rev. Biochem.* **2001**, *70*, 535.
(88) Berry, K. A.; Li, B.; Reynolds, S. D.; Barkley, R. M.; Gijón, M. A.; Hankin, J. A.; Henson, P. M.; Murphy, R. C. *J. Lipid Res.* **2011**, *52*, 1551.
(89) Veldhuizen, R.; Nag, K.; Orgeig, S.; Possmayer, F. *Biochim. Biophys. Acta* **1998**, *1408*, 90.
(90) Hallman, M.; Gluck, L. *J. Lipid Res.* **1976**, *17*, 257.
(91) Numata, M.; Chu, H. W.; Dakhama, A.; Voelker, D. R. *Proc. Natl. Acad. Sci. U.S.A.* **2010**, *107*, 320.
(92) Houtkooper, R. H.; Vaz, F. M. *Cell. Mol. Life Sci.* **2008**, *65*, 2493.
(93) Jenkins, G. M.; Frohman, M. A. *Cell. Mol. Life Sci.* **2005**, *62*, 2305.
(94) Wang, H. Y.; Jackson, S. N.; Woods, A. S. *J. Am. Soc. Mass Spectrom.* **2007**, *18*, 567.
(95) Merrill, A. H., Jr. *J. Biol. Chem.* **2002**, *277*, 25843.
(96) Hannun, Y. A.; Obeid, L. M. *Trends Biochem. Sci.* **1995**, *20*, 73.
(97) Okazaki, T.; Bielawska, A.; Bell, R. M.; Hannun, Y. A. *J. Biol. Chem.* **1990**, *265*, 15823.
(98) Masini, E.; Giannini, L.; Nistri, S.; Cinci, L.; Mastroianni, R.; Xu, W.; Comhair, S. A.; Li, D.; Cuzzocrea, S.; Matuschak, G. M.; Salvemini, D. *J. Pharmacol. Exp. Ther.* **2008**, *324*, 548.
(99) Merrill, A. H., Jr.; Sullards, M. C.; Allegood, J. C.; Kelly, S.; Wang, E. *Methods* **2005**, *36*, 207.
(100) Nakane, M.; Kubota, M.; Nakagomi, T.; Tamura, A.; Hisaki, H.; Shimasaki, H.; Ueta, N. *Neurosci. Lett.* **2000**, *296*, 89.
(101) Koval, M.; Pagano, R. E. *Biochim. Biophys. Acta* **1991**, *1082*, 113.

(102) Merrill, A. H., Jr.; Schmelz, E. M.; Dillehay, D. L.; Spiegel, S.; Shayman, J. A.; Schroeder, J. J.; Riley, R. T.; Voss, K. A.; Wang, E. *Toxicol. Appl. Pharmacol.* **1997**, *142*, 208.
(103) Milhas, D.; Clarke, C. J.; Hannun, Y. A. *FEBS Lett.* **2010**, *584*, 1887.
(104) Eibisch, M.; Schiller, J. *Rapid Commun. Mass Spectrom.* **2011**, *25*, 1100.
(105) Ishizuka, I. *Prog. Lipid Res.* **1997**, *36*, 245.
(106) Honke, K.; Zhang, Y.; Cheng, X.; Kotani, N.; Taniguchi, N. *Glycoconj. J.* **2004**, *21*, 59.
(107) Marcus, J.; Honigbaum, S.; Shroff, S.; Honke, K.; Rosenbluth, J.; Dupree, J. L. *Glia* **2006**, *53*, 372.
(108) Tadano-Aritomi, K.; Hikita, T.; Fujimoto, H.; Suzuki, K.; Motegi, K.; Ishizuka, I. *J. Lipid Res.* **2000**, *41*, 1237.
(109) Buschard, K.; Josefsen, K.; Hansen, S. V.; Horn, T.; Marshall, M. O.; Persson, H.; Mansson, J. E.; Fredman, P. *Diabetologia* **1994**, *37*, 1000.
(110) Fujimoto, H.; Tadano-Aritomi, K.; Tokumasu, A.; Ito, K.; Hikita, T.; Suzuki, K.; Ishizuka, I. *J. Biol. Chem.* **2000**, *275*, 22623.
(111) Yoda, Y.; Gasa, S.; Makita, A.; Fujioka, Y.; Kikuchi, Y.; Hashimoto, M. *J. Natl. Cancer Inst.* **1979**, *63*, 1153.
(112) Kobayashi, T.; Honke, K.; Kamio, K.; Sakakibara, N.; Gasa, S.; Miyao, N.; Tsukamoto, T.; Ishizuka, I.; Miyazaki, T.; Makita, A. *Br. J. Cancer* **1993**, *67*, 76.
(113) Liu, Y.; Chen, Y.; Momin, A.; Shaner, R.; Wang, E.; Bowen, N. J.; Matyunina, L. V.; Walker, L. D.; McDonald, J. F.; Sullards, M. C.; Merrill, A. H., Jr. *Mol. Cancer* **2010**, *9*, 186.
(114) Marsching, C.; Eckhardt, M.; Grone, H. J.; Sandhoff, R.; Hopf, C. *Anal. Bioanal. Chem.* **2011**, *401*, 53.
(115) Goto-Inoue, N.; Hayasaka, T.; Zaima, N.; Setou, M. *Glycobiology* **2009**, *19*, 950.
(116) Maccioni, H. J.; Quiroga, R.; Ferrari, M. L. *J. Neurochem.* **2011**, *117*, 589.
(117) Agranoff, B. W.; Benjamins, J. A.; Hajra, A. K. Lipids. In *Basic Neurochemistry*; Siegel, G. J., Agranoff, B. W., Albers, R. W., Fisher, S. K., Uhler, M. D., Eds.; Lippincott-Raven: Philadelphia, PA, 1999; Chapter 3; http://www.ncbi.nlm.nih.gov/books/NBK20385/ (accessed Aug 23, 2011).
(118) Boggs, J. M.; Gao, W.; Zhao, J.; Park, H. J.; Liu, Y.; Basu, A. *FEBS Lett.* **2010**, *584*, 1771.
(119) Schueler, U. H.; Kolter, T.; Kaneski, C. R.; Zirzow, G. C.; Sandhoff, K.; Brady, R. O. *J. Inherited Metab. Dis.* **2004**, *27*, 649.
(120) Sohn, H.; Kim, Y. S.; Kim, H. T.; Kim, C. H.; Cho, E. W.; Kang, H. Y.; Kim, N. S.; Kim, C. H.; Ryu, S. E.; Lee, J. H.; Ko, J. H. *FASEB J.* **2006**, *20*, 1248.
(121) Ledeen, R.; Wu, G. *J. Neurochem.* **2011**, *116*, 714.
(122) Ivleva, V. B.; Sapp, L. M.; O'Connor, P. B.; Costello, C. E. *J. Am. Soc. Mass Spectrom.* **2005**, *16*, 1552.
(123) Hunnam, V.; Harvey, D. J.; Priestman, D. A.; Bateman, R. H.; Bordoli, R. S.; Tyldesley, R. *J. Am. Soc. Mass Spectrom.* **2001**, *12*, 1220.
(124) Taban, I. M.; Altelaar, A. F.; van der Burgt, Y. E.; McDonnell, L. A.; Heeren, R. M.; Fuchser, J.; Baykut, G. *J. Am. Soc. Mass Spectrom.* **2007**, *18*, 145.
(125) Chen, Y.; Allegood, J.; Liu, Y.; Wang, E.; Cachon-Gonzalez, B.; Cox, T. M.; Merrill, A. H., Jr.; Sullards, M. C. *Anal. Chem.* **2008**, *80*, 2780.
(126) Cornett, D. S.; Frappier, S. L.; Caprioli, R. M. *Anal. Chem.* **2008**, *80*, 5648.
(127) Sugiura, Y.; Shimma, S.; Konishi, Y.; Yamada, M. K.; Setou, M. *PLoS One.* **2008**, *3*, e3232.
(128) Valdes-Gonzalez, T.; Goto-Inoue, N.; Hirano, W.; Ishiyama, H.; Hayasaka, T.; Setou, M.; Taki, T. *J. Neurochem.* **2011**, *116*, 678.
(129) Goto-Inoue, N.; Hayasaka, T.; Sugiura, Y.; Taki, T.; Li, Y. T.; Matsumoto, M.; Setou, M. *J. Chromatogr., B* **2008**, *870*, 74.
(130) Fuchs, B.; Nimptsch, A.; Suss, R.; Schiller, J. *J. AOAC Int.* **2008**, *91*, 1227.
(131) Vidova, V.; Pol, J.; Volny, M.; Novak, P.; Havlicek, V.; Wiedmer, S. K.; Holopainen, J. M. *J. Lipid Res.* **2010**, *51*, 2295.
(132) Al-Saad, K. A.; Zabrouskov, V.; Siems, W. F.; Knowles, N. R.; Hannan, R. M.; Hill, H. H., Jr. *Rapid Commun. Mass Spectrom.* **2003**, *17*, 87.
(133) Gidden, J.; Liyanage, R.; Durham, B.; Lay, J. O., Jr. *Rapid Commun. Mass Spectrom.* **2007**, *21*, 1951.
(134) Smith, D. F.; Aizikov, K.; Duursma, M. C.; Giskes, F.; Spaanderman, D. J.; McDonnell, L. A.; O'Connor, P. B.; Heeren, R. M. *J. Am. Soc. Mass Spectrom.* **2011**, *22*, 130.
(135) Hsu, F. F.; Turk, J. *J. Am. Soc. Mass Spectrom.* **1999**, *10*, 587.
(136) McAnoy, A. M.; Wu, C. C.; Murphy, R. C. *J. Am. Soc. Mass Spectrom.* **2005**, *16*, 1498.
(137) Hayasaka, T.; Goto-Inoue, N.; Zaima, N.; Kimura, Y.; Setou, M. *Lipids* **2009**, *44*, 837.
(138) Wang, H. Y.; Liu, C. B.; Wu, H. W. *J. Lipid Res.* **2011**, *52*, 840.
(139) Hart, P. J.; Francese, S.; Claude, E.; Woodroofe, M. N.; Clench, M. R. *Anal. Bioanal. Chem.* **2011**, *401*, 115.
(140) Fuchs, B.; Schiller, J.; Suss, R.; Zscharnack, M.; Bader, A.; Muller, P.; Schurenberg, M.; Becker, M.; Suckau, D. *Anal. Bioanal. Chem.* **2008**, *392*, 849.
(141) Zaima, N.; Goto-Inoue, N.; Adachi, K.; Setou, M. *J. Oleo Sci.* **2011**, *60*, 93.
(142) Guittard, J.; Hronowski, X. L.; Costello, C. E. *Rapid Commun. Mass Spectrom.* **1999**, *13*, 1838.
(143) Goto-Inoue, N.; Hayasaka, T.; Taki, T.; Gonzalez, T. V.; Setou, M. *J. Chromatogr., A* **2009**, *1216*, 7096.
(144) Wolstenholme, R.; Bradshaw, R.; Clench, M. R.; Francese, S. *Rapid Commun. Mass Spectrom.* **2009**, *23*, 3031.
(145) Bauer, J. A.; Chakravarthy, A. B.; Rosenbluth, J. M.; Mi, D.; Seeley, E. H.; De, M. G.-I.; Olivares, M. G.; Kelley, M. C.; Mayer, I. A.; Meszoely, I. M.; Means-Powell, J. A.; Johnson, K. N.; Tsai, C. J.; Ayers, G. D.; Sanders, M. E.; Schneider, R. J.; Formenti, S. C.; Caprioli, R. M.; Pietenpol, J. A. *Clin. Cancer Res.* **2010**, *16*, 681.
(146) Oppenheimer, S. R.; Mi, D.; Sanders, M. E.; Caprioli, R. M. *J. Proteome Res.* **2010**, *9*, 2182.
(147) Dobrzynska, I.; Szachowicz-Petelska, B.; Sulkowski, S.; Figaszewski, Z. *Mol. Cell. Biochem.* **2005**, *276*, 113.
(148) Sakakibara, N.; Gasa, S.; Kamio, K.; Makita, A.; Koyanagi, T. *Cancer Res.* **1989**, *49*, 335.
(149) Makhlouf, A. M.; Fathalla, M. M.; Zakhary, M. A.; Makarem, M. H. *Int. J. Gynecol. Cancer* **2004**, *14*, 89.
(150) Willems, S. M.; van, R. A.; van, Z. R.; Deelder, A. M.; McDonnell, L. A.; Hogendoorn, P. C. *J. Pathol.* **2010**, *222*, 400.
(151) Enomoto, H.; Sugiura, Y.; Setou, M.; Zaima, N. *Anal. Bioanal. Chem.* **2011**, *400*, 1913.
(152) Koizumi, S.; Yamamoto, S.; Hayasaka, T.; Konishi, Y.; Yamaguchi-Okada, M.; Goto-Inoue, N.; Sugiura, Y.; Setou, M.; Namba, H. *Neuroscience* **2010**, *168*, 219.
(153) Deeley, J. M.; Hankin, J. A.; Friedrich, M. G.; Murphy, R. C.; Truscott, R. J.; Mitchell, T. W.; Blanksby, S. J. *J. Lipid Res.* **2010**, *51*, 2753.
(154) Kobayashi, Y.; Hayasaka, T.; Setou, M.; Itoh, H.; Kanayama, N. *Placenta* **2010**, *31*, 245.
(155) Chen, R.; Hui, L.; Sturm, R. M.; Li, L. *J. Am. Soc. Mass Spectrom.* **2009**, *20*, 1068.
(156) Sugiura, Y.; Konishi, Y.; Zaima, N.; Kajihara, S.; Nakanishi, H.; Taguchi, R.; Setou, M. *J. Lipid Res.* **2009**, *50*, 1776.
(157) Matsumoto, J.; Sugiura, Y.; Yuki, D.; Hayasaka, T.; Goto-Inoue, N.; Zaima, N.; Kunii, Y.; Wada, A.; Yang, Q.; Nishiura, K.; Akatsu, H.; Hori, A.; Hashizume, Y.; Yamamoto, T.; Ikemoto, K.; Setou, M.; Niwa, S. *Anal. Bioanal. Chem.* **2011**, *400*, 1933.
(158) Hayasaka, T.; Goto-Inoue, N.; Sugiura, Y.; Zaima, N.; Nakanishi, H.; Ohishi, K.; Nakanishi, S.; Naito, T.; Taguchi, R.; Setou, M. *Rapid Commun. Mass Spectrom.* **2008**, *22*, 3415.
(159) Lohmann, C.; Schachmann, E.; Dandekar, T.; Villmann, C.; Becker, C. M. *J. Neurochem.* **2010**, *114*, 1119.
(160) Garrett, T. J.; Yost, R. A. *Anal. Chem.* **2006**, *78*, 2465.
(161) Zaima, N.; Matsuyama, Y.; Setou, M. *J. Oleo Sci.* **2009**, *58*, 267.
(162) Zaima, N.; Sasaki, T.; Tanaka, H.; Cheng, X. W.; Onoue, K.; Hayasaka, T.; Goto-Inoue, N.; Enomoto, H.; Unno, N.; Kuzuya, M.; Setou, M. *Atherosclerosis* **2011**, *217*, 427.

(163) Goodwin, R. J.; Pitt, A. R.; Harrison, D.; Weidt, S. K.; Langridge-Smith, P. R.; Barrett, M. P.; Logan, M. C. *Rapid Commun. Mass Spectrom.* **2011**, *25*, 969.
(164) Jackson, S. N.; Wang, H. Y.; Woods, A. S. *J. Am. Soc. Mass Spectrom.* **2007**, *18*, 17.
(165) Roy, M. C.; Nakanishi, H.; Takahashi, K.; Nakanishi, S.; Kajihara, S.; Hayasaka, T.; Setou, M.; Ogawa, K.; Taguchi, R.; Naito, T. *J. Lipid Res.* **2011**, *52*, 463.